SCALE-UP OF PHARMACEUTICAL TWIN-SCREW WET GRANULATION
BASED ON THE PROCESS SIMULATION USING GENETIC PROGRAMMING

SCALE-UP OF PHARMACEUTICAL TWIN-SCREW WET GRANULATION
BASED ON THE PROCESS SIMULATION USING GENETIC PROGRAMMING

By

SUMON MOZUMDER

A Thesis
Submitted to the School of Graduate Studies
In Partial Fulfillment of the Requirements
For the Degree
Master of Applied Science in Chemical Engineering

McMaster University

MASTER OF APPLIED SCIENCE (2023)   McMaster University

Chemical Engineering   Hamilton, Ontario

TITLE: Scale-up of pharmaceutical twin-screw wet granulation based on the process
       simulation using genetic programming

AUTHOR: Sumon Mozumder, B.Sc. Eng., M.Eng.

SUPERVISOR: Dr. Michael R. Thompson

NUMBER OF PAGES: xii, 65

LAY ABSTRACT

Granulation is considered as a common size enlargement process for tableting that has attracted much attention in pharmaceutical manufacturing because of its ability to improve granule flowability and ensure consistency in the granule properties. This study used continuous wet granulation on the two most popular sizes of twin-screw extruders. Granulation experiments at a range of different conditions were performed on the two extruders to produce granules, which were then characterized for determining granule properties. This study mainly focused on the possibility of scaling up between the two extruders without changing the final granule properties and used an Artificial intelligence tool to develop mathematical models for both extruders to predict granule properties. These mathematical models were beneficial to establish scaling rules for the granulation system.

ABSTRACT

Wet granulation is a crucial process in the manufacturing of pharmaceutical tablets. For several years, twin-screw wet granulation has been noticeably studied as a continuous method for granulation in the pharmaceutical industry because of its ability for producing uniform granules with greater flowability and consistency. Some big challenges still exist in controlling the desired granule properties when different-sized extruders are used in product development. Introducing new technology to the Quality-by-Design approach and scaling up a wet granulation system on the twin-screw extruder demands a robust process understanding and improvement of knowledge by studying the dominance of critical process parameters on the properties of the granules. Therefore, it was vital to study the possibility of scaling up between different-sized twin-screw extruders and observe the effect of variations in the process concerning granule properties.

The current study intended to understand the behavior of the wet granulation process in the two popular sizes of twin-screw extruders used in pharmaceutical manufacturing, 18 mm, and 27 mm. Two key dimensionless groups, the Reynolds number, and the Péclet number were studied to evaluate their impact on the flow behavior and mixing performance during wet granulation of a sustained released formulation. It was realized that the two dimensionless groups exhibited inconsistent effects on granule properties, including the upper moment (d_{90}) and span of the particle size distribution and granule fracture strength. In this study, the influence of material flow, residence time distribution, degree of channel fill, and mixing intensity on the wet granulation process were explored in detail for both extruders. The higher influence of the Péclet number on wet granulation was greatly dependent on the degree of fill,

whereas the Reynolds number had the least effect on the residence time distribution and mixing performance.

The significance of the fill level for scale-up on the twin-screw extruder was huge to ensure steady mixing during granulation and reduce variation in the product. The interaction between the screw speed and the material feed rate was therefore examined with particular focus on the resultant fill level and a method was suggested for quantifying the degree of fill for the two extruders. It was noticed that variation in the free channel space greatly influenced the properties of the granules when produced from the two different-sized extruders. Hence, the degree of fill and scale of the twin-screw extruder had a very significant effect on the granule properties. Genetic programming was employed as an Artificial intelligence tool for modeling the granule properties which developed valuable mathematical equations. These equations were very useful for establishing important scaling laws for the wet granulation system on the twin-screw extruder.

ACKNOWLEDGEMENTS

Table of Contents

LIST OF TABLES

LIST OF FIGURES

x

xi

LIST OF ACRONYMS

API - Active Pharmaceutical Ingredient
CPP - Critical Process Parameter
CQA - Critical Quality Attribute
DF - Degree of Fill
DOE - Design of Experiments
FDA - Food and Drug Administration
Fr - Froude Number
GP - Genetic Programming
HSG - High Shear Granulation
HMG - Hot Melt Granulation
L/D - Length to Diameter Ratio
LSR - Liquid-to-Solid Ratio
MRT - Mean Residence Time
MLR - Multiple Linear Regression
PSD - Particle Size Distribution
Pe - Péclet Number
PFR - Powder Feed Rate
PFN - Powder Feed Number
QbD - Quality-by-Design
RPM - Revolution Per Minute
Re - Reynolds Number
RTD - Residence Time Distribution
RSE - Relative Standard Error
SS - Screw Speed
SR - Symbolic Regression
TSE - Twin Screw Extruder
TSG - Twin Screw Granulation
TSWG - Twin Screw Wet Granulation
We - Weber Number

CHAPTER 1: INTRODUCTION

1.1 Background

For pharmaceutical companies, knowledge of their manufacturing processes and the influences of these processes on intermediate and final product properties is critical to achieving the high quality needed. For this reason, regulatory agencies (FDA) and pharmaceutical manufacturing companies started many initiatives in recent years to improve process understanding and expand continuous manufacturing, which is more consistent [1]. One of three common manufacturing methods, such as direct compression, dry granulation, and wet granulation, usually makes solid oral pharmaceutical products, though the latter is more common [1], [2]. In pharmaceutical manufacturing, granulation is a widely used technique for combining one or more powdered particles through compression or using binding liquid to produce larger solids. It is a crucial step in processing to improve flowability and compressibility for tableting [3].

Previously, batch processes with low and high shear involved wet granulation, though continuous wet granulation is growing in popularity because of its many advantages [4]. Twin-screw granulation is a faster process than any other method by being continuous, which results in increased productivity, less product rejection/waste, greater flexibility in the output quantity, and better in-process control [3], [5]. It also has reduced residence time when compared to a conventional wet granulation with a high-shear batch mixer [6], [7]. Meeting throughput rate targets demand a necessary scale of the equipment [7], which can alter granule properties unless subsequent changes occur to the processing parameters. Several recent studies have highlighted the impacts of different process parameters on the granulation mechanism (nucleation, growth,

and breakage) but the influence of the size of the extruder is most responsible for varying the product quality [8]–[10].

Twin screw wet granulation (TSWG) involves several physical and chemical phenomena, and it is essential to realize what happens in the granulation process when the size of the extruder changes. The scalability of TSWG is incredibly challenging and only a few studies are available up to the present time. Hence, developing a viable scaling method is beneficial to scale up a wet granulation system in twin-screw extruders and improve our understanding of the process. An effective scaling-up method is vital for sustaining reliability in the granulation process and producing uniform granules over time [1]. One of the major challenges is to consider appropriate dimensionless numbers for scaling up a granulation system. Considering the multiple mechanisms involved, different dimensionless numbers were involved in developing an appropriate scaling rule.

The present scale-up study considered two dimensionless numbers, such as Reynolds number (Re) and Péclet number (Pe), to examine their influences on the upper moment (d_{90}) and span of the particle size distribution (PSD), and fracture strength of granules produced. Genetic programming (GP) seemed to be a highly attractive route to develop the scaling rules based on process data collected experimentally. This scaling work maintained geometric similarity between two different sizes of granulators, whereas the setting of the operating process parameters based on two dimensionless numbers (Re and Pe) maintained kinetic and dynamical similarities. As included in this study, the filling level in a smaller and larger twin-screw granulator seemed like another dimensionless number for explaining the kinetic conditions inside the granulators, which was statistically modeled for changing powder feed rate and screw speed.

2

1.2 Objectives of the Thesis

The objective of the thesis was to develop and evaluate scaling rules for a continuous twin-screw wet granulation process using two sizes of twin-screw granulators.

The specific objectives are as follows:

- Determine the mean residence time from the residence time distribution and build a statistical model based on the process parameters to predict the degree of fill for the different-sized granulators.

- Develop an artificial intelligence tool based on the process, and based on the particle size (d_{90}), span, and granule fracture strength.

- Establish scaling rules for the granulators varying in capacity and reducing the dependency on the experimentation.

CHAPTER 2: LITERATURE REVIEW

2.1 Granulation

Granulation is a crucial technique for tableting that transforms fine particles into strong and large agglomerates. This process improves the flowability and compressibility of granules, reduces segregation and dusting, and increases homogeneity in the material. The granulation process also eliminates excess fine particles to minimize tablet defects, improve productivity, and reduce manufacturing time [1]–[3], [11], [12]. Pharmaceuticals are usually made by one of three important granulation methods: dry, wet, and hot melt granulation (HMG), though pharmaceutical companies mostly use wet granulation to produce drugs because of its numerous benefits [2], [13], [14]. Dry granulation involves powder compression by a roller, whereas wet granulation needs a granulating liquid or a binder solution to bind excipients and active pharmaceutical ingredients (APIs) together [3]. In dry granulation, mechanical interlocking, cohesion, and van der Waals forces create inter-particle bonding because of the application of pressure or mechanical forces to the powder bed.

HMG has an especially high interest in continuous granulation using twin-screw extruders (TSEs) because of the machine's capacity to handle the heat. This type of granulation uses a molten binder (wax, lipid, or polymer) in the process to form liquid bridges between the solid particles while heated above its softening or melting point. Upon solidification, these bridges harden when they cool down to ambient conditions upon exiting the extruder barrel [5], [15]; using a waxy binder improves the flowability of granules, though it can increase the required strength. For this granulation, the process temperature should be lower than the melting point of the API, but higher than the glass transition temperature of the binders [10].

Both hot melt and dry granulation are popular for moisture-sensitive formulations, whereas wet granulation is suitable for producing thermally sensitive drugs.

Mechanisms of wet (and HMG) processes include three basic steps such as wetting & nucleation, consolidation & growth, and breakage & attrition [16] though all these steps do not essentially take place at the same time nor to the same degree based on the method used. The conventional batch process involves the last two steps happening concurrently, which presents hurdles in controlling the granule properties. The continuous twin-screw granulation process has improved control over the resulting granule properties since there is a visible separation between the wetting & nucleation step and the consolidation & growth step [16]. Initially, nuclei form depending on the viscosity of the binder and the binder droplet size relative to the initial solid particle. With higher binder viscosity, the immersion mechanism controls the nucleation step, whereas the distribution mechanism dominates nuclei formation when the binder droplet size is relatively small compared to the particles [5]. Growth is a crucial step, and it typically takes place when the size of nuclei begins to increase [5]. In twin-screw granulation (TSG), coalescence is vital for granule formation and depends on the degree of liquid dispersion or saturation. The consolidation of particles, which depends on the capillary and mechanical forces during the mixing process, can increase the liquid dispersion. Granule breakage depends on the wet granular strength and mechanical stress from the twin-screw extruder (TSE). Usually, granules having greater strength withstand breakage under specific mechanical conditions, though extreme mechanical force can break the granules [5]. The combined actions of capillary force, viscous force, and inter-particle frictional force are essential to developing granular strength. Viscous force regulates the dynamic granular strength, whereas capillary force results in steady granule strength. The viscosity of the binder

5

causes viscous forces, whereas the capillary force depends on the force due to surface tension and the interaction between the liquid binder and solid particles [5].

2.2 Continuous Wet Granulation in Twin-Screw Extruder

TSG is getting significant attention in pharmaceutical manufacturing for its continuous operations, as it improves both production efficiency and equipment flexibility. Compared to traditional granulation methods, twin-screw wet granulation (TSWG) is a more effective technique for producing a high quantity of consistent granular particles [9], [17]. Being continuous process, TSG offers more output, fewer batch refusals, reduced production cost, greater flexibility in batches, and better in-process monitoring and control [18]–[20]. In other words, in-process monitoring of TSG helps to control the desire properties of granules without causing any defects that results more productivity and less wastage of material. The granules produced by TSG have a notably lower fracture strength when compared to those from a high-shear batch mixer; granules formed by TSEs are highly compressible because of their porous structure, and tablets made by these granules tend to have high tensile strength (which is desirable).

In TSG, granule properties mainly depend on formulation, binder selection, and process parameters [3], [21], [22]. The relationships between different extrusion parameters such as powder feed rate, screw speed, barrel temperature, and screw geometry largely affect mixing intensity, residence time, powder compression, particle size distribution (PSD), exit temperature, and so forth [18], [22]. System parameters, including residence time distribution (RTD) and screw torque, also have a correlated influence on the properties of granules [21]. In TSWG, the liquid-to-solid (L/S) ratio is the most influential factor regarding granule quality [23]. Other factors such as a higher barrel temperature or higher powder feed rate can result in

6

larger granules by twin-screw wet granulation [24]. Denghe et al. [23] reported that the median

particle size (d_{50}) of granules reduced with an increase in powders feed rate and screw speed,

but also found the fracture strength of granules increased with powders feed rate and L/S ratio.

Other studies revealed that a higher powders feed rate and greater viscosity of a granulation

liquid resulted in longer residence times, more barrel fill, and higher torque. It also produced

spherical, stronger, and denser granules with a narrower PSD [25]–[28]. Increasing the powder

feed rate can promote more capillary action that forms larger granules, though it also depends

on the screw speed. Some authors pointed out that screw speed influenced the residence time

and granular growth, since a higher screw speed led to lower compaction of the granules,

shorter residence time, narrower particle size distribution, and produced larger granules [27],

[29], [30]. Thus, the changes in screw speed, powders feed rate, and L/S ratio had a meaningful

impact on the residence time and the average torque during the granulation process.

A suitable screw design is essential for the granulation, as the kneading block

compresses agglomerates to form denser and stronger granules. A kneading block where its

discs are at a larger offset angle provides the highest shear to the material [31]–[34]. One study

reported that increasing the number of kneading elements led to more friction inside the barrel

and consequently resulted in higher torque values. The angle of the kneading disc usually had

no important effect on the torque and only became important when TSWG used a higher

number of kneading elements. According to another study, the angle of kneading elements only

affected the PSD when the barrel filling degree was high (70%) [7]. Other authors highlighted

the impact of screw configuration on PSD, where conveying elements produced wide

multimodal size distributions while kneading elements reduced granule size [35]. Three

different screw geometries consisting of an incremental number of kneading blocks were tested

in another granulation study, where granule size was reduced but fracture strength increased

because of escalation in the residence time and axial dispersion inside the twin-screw extruder [36]. It was also pointed out that implementing an extra conveying element after the kneading block improved the granulation yield by reducing the oversized agglomerates [32].

2.3 Scale-Up of Granulation in Twin-Screw Extruder

Scale-up of TSG is beneficial to its optimization and makes for a more cost-effective process, allowing the shifting from smaller-scale equipment to larger versions while maintaining at least one important attribute as fixed [37]. It is essential to know how machine size affects granulation since the process involves many unit operations, such as melting, mixing, nucleation, agglomeration, and breakage [37]. Understanding scale-up is also essential to Quality-by-Design (QbD) where process parameters control the desired granule quality [37]. Developing an efficient scaling-up method for TSWG can be challenging because critical process parameters (CPPs) will control the quality attributes of granulation. It is crucial to identify the most dominating parameters of the process that have an important impact on the critical quality attributes (CQAs) [28].

Developing the design space governing granule quality requires many TSWG experiments and that demands time and great expense when done on a production-sized machine. Therefore, it is better to conduct experiments first in a smaller extruder and then scale up the process efficiently. The optimal design space allows a TSWG process to be less sensitive to slight changes in parameters. The underlying goal of a scale-up strategy is to ensure particles experience the same mechanical stresses within different scales of equipment to produce identical granules. By maintaining geometry, dynamical, and kinematic similarity, it is possible to achieve scale-up for a continuous TSWG. There are two scale-up philosophies, macroscopic and microscopic, though the latter emphasizes process understanding to ensure consistency in

8

the process and establishes a workable scale-up [38]. In a macroscopic scale-up approach, the process involves regulating parameters on various scales to get desired granule quality through in-process measurements [39]. In a microscopic approach, conducting several experiments on small-scale equipment improves process knowledge to identify the critical process parameters (CPPs), and then scaling rules help in defining parameter values at the larger version to maintain the quality of the granules [40]. Both scale-up strategies have some limitations, though a hybrid approach can increase the possibility of an efficient scale-up for any granulation system. A few scale-up studies of TSWG were done, but these studies were not fully successful because of some limitations. Djuric et al. [16] performed a comparative study of granulation for two different sizes of TSG to evaluate the impact of powder feed rate and screw speed on granule properties. The authors reported that the smaller TSG yielded a higher proportion of fines, whereas the larger TSG formed more coarse granules. They observed that the influence of powder feed rate on granule size was more apparent on the larger TSG. The study considered the Froude number (Fr) as a dimensionless number but did not involve dimensional similarity or any proposed scaling rules [16]. As a result, the flow rates and screw speeds examined between the two different sizes of extruders did not consider them in suitably scaled ranges to identify any scaling trends. Another study proposed three key scale-independent dimensionless groups, such as Froude number (Fr), Powder feed number (PFN), and Liquid-to-solid ratio (LSR) would be appropriate to scale up granulation across three different sizes of TSG maintaining geometric similarity [1]. The study revealed that the LSR affected PSD, whereas Fr and PFN only correlated with the higher moment of the particle size distribution (d90). There were no trends found with granule porosity according to this study. The authors of the study pointed out that larger TSG yielded less breakage of coarse granules because of the larger gap between the screw and the barrel's inner surface. Further studies related to the scalability of TSG have considered three geometrically similar TSGs, but the

9

authors in that study identified no dimensionless numbers in their selection of operating conditions [41]. Their study involved RTD and DF and reported that the interaction at a very low DF, wider RTD, or higher L/S ratio substantially impacted particle size and density [41]. Screw channel filling was an important factor when comparing different sizes of TSG, though the author did not mention any method to quantify the degree of filling. Screw configuration, DF, and RTD are very crucial to scale-up, but up to the present, no particular and persuasive quantification methods exist for DF [42]. The impact of residence time on the transformation of the product is obvious, and RTD in a TSE can be a favorable tool to scale up and determine optimal process conditions. Another study related to regime maps for different granulation processes considered two dimensionless numbers, such as Reynolds number (Re) and Weber number (We), to differentiate spreading and granular growth, which led to a reduction in both the experimental workload and the number of parameters to be considered [42]. Other authors included Péclet number (Pe) in a wet granulation study and the results revealed that screw speed was the most important parameter in terms of RTD and axial mixing in the TSG [6].

However, previous scale-up studies rarely considered Re and Pe on the scaling of TSWG, and using these dimensionless numbers on different TSG scales, can estimate the granule properties. Re is an important dimensionless number to understand the flow behavior of powdered particles in the extruder, and its calculation requires the characteristic diameter, axial velocity of flow, and viscosity of the wet powder. It is difficult to determine the actual mixing intensity during TSWG, but the Pe can be a good index for axial mixing in the extruder, which can estimate its impact on granule size and fracture strength.

2.4 Genetic Programming

Genetic programming (GP) is a potential evolutionary approach for extracting knowledge, and it is an optimization tool for finding an optimal solution for complex problems. This modeling approach was widely used to uncover analytical expressions descriptive of observed datasets of input and output values. GP models predicted outputs for a system more efficiently than any other numerical method [43]–[45]. One study revealed that a GP model had superior prediction ability compared to statistical DOE regression technique or multiple linear regression (MLR)-based polynomial models [43]. A GP model offers parametric equations, which are simple to explain and examine, and this model has a greater ability to understand the fundamental mechanisms of the modeled process [43], [45]. In symbolic regression by genetic programming, populations comprise equations generated based on the Darwinian principle of survival of the fittest [44]–[46].

The symbolic regression technique can develop an efficient GP model, where a tree diagram displays the structure of the individuals representing mathematical equations [47]. The internal nodes or points of the tree are functions or operations, whereas the peripheral points are terminals or input data. A GP architecture combines different arithmetic operations (+, −, *, /, and so forth), and mathematical functions (sin, cos, tan, log, exp, sqrt, and so forth) and involves model parameters to provide an optimal equation [47]–[51]. There are five important phases of GP modeling such as population initialization, fitness function, selection, crossover, and mutation [52], [53]. Several numerical expressions generated by GP programming depend on the initiation of a random population and the setting of termination criteria. A fitness function is important to evaluate each mathematical equation where the lowest positive or zero value show the best fitness. Tournament size selects the suitable equations for crossover and mutation based on the fitness values. Crossover helps to generate new equations by exchanging

operations and functions between the existing mathematical equations, whereas mutation results in diversity in the new equations to achieve an optimal solution [43], [46], [54].

Some authors pointed out that the traditional methods required many experimentations to make controlled-release drug delivery systems, where the GP model optimized pharmaceutical formulation problems by deriving important mathematical expressions based on the reduced experimental data [43]. In other studies, the GP model proved to be an effective and efficient tool for modeling various controlled release formulations, where GP automatically generated some equations to describe the cause-and-effect relationships in a system [44], [55], [56]. Thus, GP is a valuable and useful tool for developing controlled-release formulations because of its predictive power, reliability, and simplicity. Another study considered the GP to scale up a high-shear wet granulation process for the modeling of the granulation process for granulators of similar and dissimilar geometries and predicting the endpoint of the granulation process by developing a set of mathematical equations [57]. Besides, GP developed important equations in the field of microfiltration of oil-in-water emulsions to estimate the membrane fouling and predict the oil rejection rate during the operation [45]. This valuable tool was also used for predicting the filtration performances of a pilot plant for different water quality and changing operating conditions which established some mathematical equations as well [58].

However, TSWG is an efficient approach for producing uniform granules under controlled conditions and is appropriate for APIs which are thermally sensitive. Besides, a workable scaling-up method plays a meaningful role in maintaining consistency in the granulation process, which efficiently manufactures a preferred product on a larger scale. A limited piece of work helped to understand the granulation mechanisms in a TSE partially

because of the complexity of the equipment and very few studies related to the scale-up of TSWG are done up to the present time. There was also a gap in process simulation-based scaling-up studies of TSWG, which has been filled by this work.

CHAPTER 3: EXPERIMENTAL

3.1 Materials and Equipment

3.1.1 Materials

The formulation considered in this study was 60% α-lactose monohydrate (Flowlac®100; Meggle Pharma, Germany), 20% microcrystalline cellulose (Avicel PH102; Dupont Nutrition & Biosciences, Midland, MI, USA), and 20% Kollidon® SR (BASF, Florham Park, NJ). An aqueous solution of 2% METHOCEL^{TM} E3PLV (DuPont Nutrition & Biosciences; Midland, MI, USA) was used as a liquid binder in this study. Kollidon® SR is a control-released excipient that extends the release of an active pharmaceutical ingredient (API) over time within different solid oral dosage forms. The bulk density, tapped density, compressibility index, and Hausner's ratio of the formulation (powder mixture) were measured and observed as 0.57 g/cm^3, 0.81 g/cm^3, 30%, and 1.42, respectively. The powder mixture was dried each time at 50^{0}C for at least 3 hours in a convective oven before performing any granulation experiments. The moisture content of the formulation (dried) is measured on a wet basis (loss on drying) with a halogen moisture analyzer (Mettler Toledo®-HG63 series). One gram of formulation was tested in the moisture analyzer at 105°C for 5 minutes and the moisture content value was observed between 1.6% and 3.2%. Three repeats were made for each sample to estimate the uncertainty of the test.

3.1.2 Equipment

Wet granulation experiments were performed on 18 mm (MICRO-18) and 27 mm (ZSE 27 HP) co-rotating twin screw extruders (Leistritz Extrusion; Somerville, NJ, USA). The specifications of the two extruders are given in Table 3.1. The liquid binder was injected into

a twin-screw extruder at barrel zone 3 with an ISCO 260D high-pressure syringe pump (Teledyne-ISCO Inc.; Lincoln, NE, USA) whereas the powder was added into the extruder using a Brabender T20 twin-screw gravimetric feeder (Mississauga, ON, Canada). The same screw design (as shown in Figure 3.1 and Figure 3.2) was used for all wet granulation experiments for both extruders, which consists of conveying elements followed by a single kneading block with two 60^0 stagger kneading elements and subsequent conveying elements before the exit of the barrel. The screw design was the same, but the screw pitches were different to maintain the geometric similarity between the two extruders.

Table 3.1 Specification of 18 mm and 27 mm twin-screw extruders.

Nominal diameter of the screw (mm)	L/D	The maximum rotational speed of the screw (rpm)	Power consumption (kW)	Current consumption (amp)	Voltage (volt)	Frequency of motor (Hz)
18	40/1	500	2.3	12	380	60
27	40/1	600	18	16	460	60
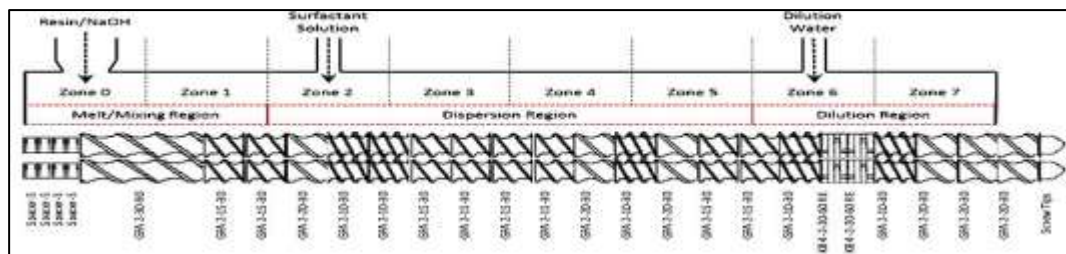
Figure 3.1. Screw design for 18 mm twin-screw extruder.
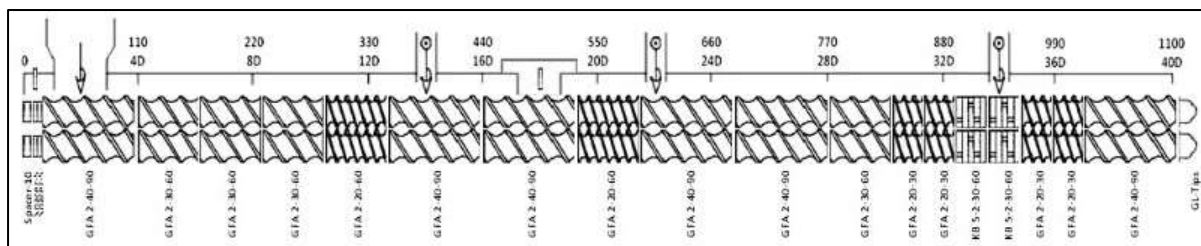
Figure 3.2. Screw design for 27 mm twin-screw extruder.

In the case of the small-size twin-screw extruder (18 mm), the barrel had a free volume of 68 cm^3, whereas for the large-size extruder (27 mm) the barrel had 304 cm^3 free space which largely affects the degree of fill inside the barrel. The barrel of the smaller extruder consisted of eight zones, whereas the larger extruder barrel contained ten zones. For all experiments, the barrel temperature was always set to 25^{0}C due to the low glass transition temperature (30-35^{0}C) of Kollidon® SR. Figure 3.3 presents a schematic diagram showing the wet granulation process on the 18 mm twin-screw extruder.

1 -Gravimetric solid feeding unit
2 -Feeding hoper
3 -Gravimetric liquid dosing pump
4 -Liquid injector
5 -Heating barrel
6 -Twin screws
7 -Extruder control panel
8 -Screw driving unit
9 -Granules exiting the extruder
10 -Granules collecting tray
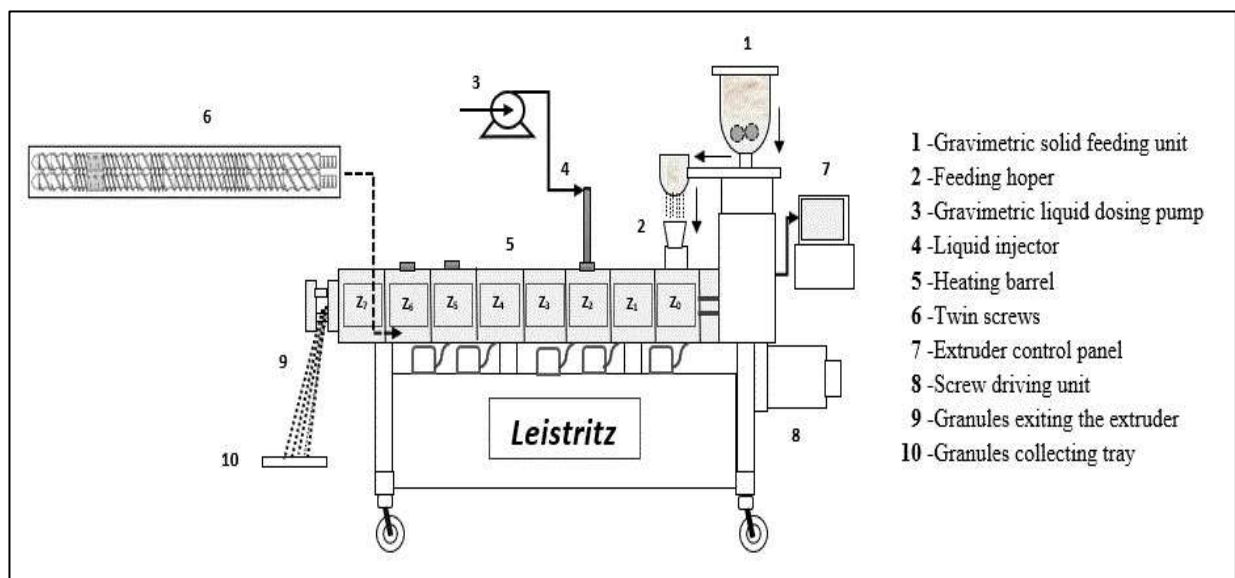
Figure 3.3. Schematic diagram showing wet granulation on18 mm twin-screw extruder.

3.2 Design of Experiments

The atmospheric temperature and relative humidity during the granulation experiments on the 18 mm twin-screw granulator were measured and recorded as 22-24^{0}C and 26-44%, whereas for the 27 mm granulator it was found as 24-26^{0}C and 10-15%, respectively.

For the 18 mm twin-screw extruder, the wet granulation experiments were performed at 26% and 30% liquid-to-solid (L/S) ratios to observe the effects of this parameter on the

scaling and granule properties, whereas all experiments on the 27 mm extruder were conducted at 26% L/S ratio; the higher L/S was not necessary to examine on the 27 mm because the extruder allows sufficient liquid saturation during granulation. A design of experiments was employed to examine the impacts of process parameters (powder feed rate and screw speed) and the size of the extruder on the granule properties. For both extruders, screw speeds and powder feed rates were varied as described in Table 3.2, Table 3.2, and Table 3.3, based on the two dimensionless parameters described in the next section. Initially, the wet granulation experiments were performed on the smaller extruder (18 mm), and then scaled up on the larger extruder (27 mm).

3.3 Developing Scaling Rules Using Dimensional Analysis

Scaling rules for granulators are commonly desired by regulatory authorities and pharmaceutical companies to maintain consistency within their processes and produce uniform granules over time. In this study, the geometric similarity was maintained between the 18 mm and 27 mm twin-screw extruders by being made by the same vendor and using identical screw designs, whereas kinetical and dynamical similarities were maintained by adjusting their processing parameters individually based on two important dimensionless numbers, the Reynolds number, and the Péclet number. These dimensionless numbers were employed to develop scaling rules and improve understanding of powder mixing and granular growth. In other words, Reynolds number (Re) and Péclet number (Pe) were maintained at the same level for both extruders to retain dynamic and kinematic similarities. In this study, the above two sizes of twin-screw extruders (TSE) were compared to assess the scalability of granule properties involving particle size distribution (PSD) with its moments (d_{90} and span), and granule fracture strength.

Process variables related to these dimensionless parameters that were varied during scaling between the two twin-screw extruders are D, L, D_h, N, U, m_p, m_l, L/S, ρ_b, μ; where D is the barrel diameter, L is the barrel length, D_h is the hydraulic diameter for the flow path, N is the screw speed, U is the axial velocity of powders, m_p and m_l are the mass flow rates of powders (formulation) and liquid, L/S is the liquid-to-solid ratio, ρ_b is the bulk density of powder mixture, ρ_l is the density and μ_l is the dynamic viscosity of liquid binder. The final granule properties which were evaluated after granulation experiments include particle size distribution (PSD) with its moments (d_{90}, span), and granule fracture strength (τ). In this study, the following functions were generated:

$$PSD(d_{90}, span) = f_1(D, L, D_h, N, U, m_p, m_l, L/S, \rho_b, \rho_l, \mu_l \dots) \qquad (1)$$

$$\tau = f_2(D, L, D_h, N, U, m_p, m_l, L/S, \rho_b, \rho_l, \mu_l \dots) \qquad (2)$$

Using the principles of dimensionless analysis, the above two equations can be rewritten as:

$$\frac{PSD(d_{90}, span)}{D} = g_1\left(Re, Pe, \frac{L}{D}, DF, \dots\right) \qquad (3)$$

$$\frac{\tau}{D} = g_2\left(Re, Pe, PFN, \frac{L}{D}, DF, \dots\right) \qquad (4)$$

where Reynolds number was calculated as:

$$Re = \frac{\rho_b U D_h}{\mu_{wp}} \qquad (5)$$

And Péclet number was determined as:

$$Pe = \frac{\rho_b U D_h^2}{m_p} \qquad (6)$$

And DF is the degree of fill, which was determined as:

$$DF = \frac{Q_m \times MRT}{V_f} \qquad (7)$$

where Q_m is the total volumetric flow rate of both powder and liquid (calculated by $\frac{m_p}{\rho_m}$ and $\frac{m_l}{\rho_l}$), V_f is the free volume of the screw, and MRT is the mean residence time, which was experimentally determined as discussed in the next section.

The viscosity of wet powders (μ_{wp}) was determined considering the rheology of particle-liquid suspensions [59], [60]. During wet granulation, when the liquid binder (liquid phase) was added to the powder bed (solid phase) it formed a suspension of powdered particles in a low-viscosity matrix. For dilute suspension (φ_s<1 and J<0) the viscosity of wet powder was calculated by:

$$\mu_{wp} = \mu_l\,(1\text{-}\frac{\varphi_s}{J}) = \mu_l\,(1\text{+}2.5\varphi_s)\,[\text{where J=-0.4}] \tag{8}$$

where μ_l is the dynamic viscosity of liquid binder (3 mPa-s), φ_s is the volume fraction of solid powders (0.84 for 26% L/S ratio and 0.82 for 30% L/S ratio) and J is the microstructural parameter which is dependent on the shape and distribution of the phases (liquid and solid).

The volume fraction of solid powders was determined as follows:

$$\varphi_s = \frac{V_s}{V_s + V_l} = \frac{\dfrac{m_p}{\rho_p}}{\dfrac{m_p}{\rho_p} + \dfrac{m_l}{\rho l}} \tag{9}$$

where V_s is the volumetric flow of powders, V_l is the volumetric flow of liquid, m_p is the powders feed rate (g/min), m_l is the liquid flow rate (ml/min), ρ_s is the bulk density of powders (0.57 g/cm^3) and ρl is the density of the binding liquid (1.08 g/cm^3).

To determine the viscosity of the wet powder, the dilute suspension model was considered because wet powder viscosity in this study had low significance and dominance for the calculation of the Reynolds number. In pharmaceutical wet granulation studies, no

appropriate method was available to quantify the viscosity of wet powder matrix and hence Einstein's viscosity equation was considered in this case as a model that handled volume of solids and the viscosity of the liquid binder even though it is meant for dilute suspensions; since the liquid-to-solid ratio was not the focus of the study (though it was varied between two states), it was felt that this model was sufficient for the calculations.

For the determination of Re and Pe, the axial velocity of powders [61] was calculated as $U = \lambda*N$; where λ is the weighted-average pitch of the screw (16 mm for the smaller extruder and 30 mm for the larger extruder). The hydraulic diameter (D_h) of the flow path was calculated as $D_h = D_o-D_i$; where D_o is the screw diameter and D_i is the diameter of the screw shaft. The value of D_h was calculated as 11 mm for the smaller extruder (18 mm) and 15 mm for the larger extruder (27 mm). The axial velocity of powders was determined based on one screw to study the segmented motion of the powders on one path.

The setup of processing parameters was made based on the above-mentioned dimensionless numbers as shown in Equations (5)-(6) and stipulated in Table 3.2, Table 3.3, and Table 3.4. The degree of fill (DF) for 18 mm and 27 mm twin-screw extruders were calculated from the mean residence time (MRT) as shown in Equation (7). For both 18 mm and 27 mm extruders, the calculated degree of fill (DF) was modeled as a regression fit for powder feed rate and screw speed to develop a predictive approach for estimating the degree of fill (DF).

Table 3.2 Design of experiments for 18 mm twin-screw extruder for 26% L/S ratio.

Exp. No.	Screw speed (rpm)	Powder feed rate (kg/h)	Re	Pe
1	100	0.5	0.180	13.242
2	100	0.8	0.180	8.276

3	100	1.1	0.180	6.019
4	100	1.4	0.180	4.729
5	200	1.0	0.360	13.242
6	200	1.6	0.360	8.276
7	200	2.2	0.360	6.019
8	200	2.8	0.360	4.729
9	300	1.5	0.541	13.242
10	300	2.4	0.541	8.276

Table 3.3 Design of experiments for 18 mm twin-screw extruder for 30% L/S ratio.

Exp. No.	Screw speed (rpm)	Powder feed rate (kg/h)	Re	Pe
1	100	0.5	0.184	13.242
4	100	1.4	0.184	4.729
5	200	1.0	0.367	13.242
8	200	2.8	0.367	4.729

Table 3.4 Design of experiments for 27 mm twin-screw extruder for 26% L/S ratio.

Exp. No.	Screw speed (rpm)	Powder feed rate (kg/h)	Re	Pe
1	39	0.7	0.180	13.242
2	39	1.9	0.180	4.729
3	78	1.4	0.360	13.242
4	78	3.8	0.360	4.729
5	117	2.0	0.541	13.242
6	117	5.7	0.541	4.729

Each experiment described in Table 3.2, Table 3.3, and Table 3.4 had three samples collected from the exit of the extruder to be used as repeats for assessment of uncertainty. In the design of experiments, the Reynolds number (Re) and Péclet number (Pe) were selected based on the physical operating limits of the machine; higher Re or lower Pe would create jamming problem for the 18 mm twin-screw extruder, which had less available space inside the barrel for powder.

3.4 Measurement of Residence Time

Residence time distribution (RTD) was measured to examine the axial mixing for both twin-screw extruders. Mean residence time (MRT) was calculated from its RTD to determine the degree of fill for smaller and larger extruders. During the wet granulation experiments, two extruders were run with the same formulation at varying flow rates and screw speeds to produce granules. The extruders were stabilized for half an hour before and after performing each experiment. A camera was placed at the delivery end of the extruders to capture a stream of granules exiting the extruder barrel under fixed light conditions. After starting each experiment, the granulation process was allowed to reach a steady state for three minutes and then 0.6 grams of cocoa powder (dye tracer) was added as a pseudo-Dirac pulse into the feed zone. Initially, the existing granules were colorless and then colored with cocoa powder. The recording continued until the colored granules became colorless again. Afterward, images on a ten-second interval were extracted from each recording by a VLC media player software and then analyzed by Image J image-analysis software (NIH, USA) to determine the color intensity of every image. The color intensity was assumed to be linearly correlated with the concentration of the tracer. Mean residence time (MRT) was calculated by using the following equation.

$$MRT = \Sigma \ (t*E(t)) \tag{10}$$

where t represents the time in second and,

$$E(t) = \frac{\text{Red Intensity}_t}{\Sigma_{t=0}^{t} \text{Red Intensity}} = \frac{c(t)}{\int_0^\infty c(t)dt} \tag{11}$$

22
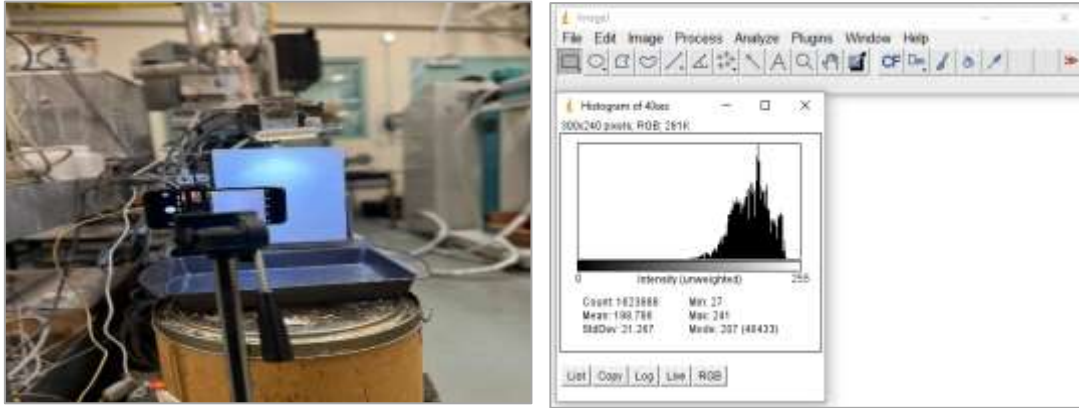
Figure 3.4. Measurement of mean residence time (MRT).

The error for the calculation of MRT was assessed by determining a relative standard error (RSE). The RSE was determined by repeated studies within the Research group using the same technique for similar granulation materials, though there was no time in this study to make those assessments.

3.5 Particle Characterization

3.5.1 Analysis of Particle Size Distribution (PSD)

Granules produced from the twin-screw extruders were collected and air-dried at room temperature for 48 hours before being analyzed for their size. A sieve shaker (ROTAP RX-29; W.S. Tyler, USA) was used to determine the PSD using a series of sieves (2100 μm, 1700 μm, 1400 μm, 1180 μm, 850 μm, 500 μm, and 300 μm nominal openings) and a bottom pan. A granulated sample of 100 grams is classified into eight size fractions based on sieve sizes by constant mechanical agitation for five minutes to ensure complete separation of the particles. Then, the retained mass on each sieve is used to determine the PSD. The span is calculated from three particle size distribution moments (d_{10}, d_{50}, and d_{90}) as follows:

$$\text{Span} = \frac{(d_{90} - d_{10})}{d_{50}} \qquad (12)$$

The errors for the calculation of moments of PSD (particle size and span) were assessed by determining a relative standard error (RSE).

3.5.2 Determining Granule Fracture Strength

Maintaining granule fracture strength is crucial for resisting pressure during compression for tableting. Moreover, the fracture strength of granules also affects the tensile strength of a tablet. In general, a tablet should have sufficient tensile strength to endure stresses caused by industrial production, shipping, and processing [62]. The Instron universal mechanical testing system was used to perform a confined uniaxial compression test on the granules to measure the compressive stress and compressive extension, which are beneficial for the calculation of fracture strength [36], [63]. A model 3366 bench-top mechanical testing system (Instron Corporation; Cantor, MA, USA) with a 5 KN load cell was used to determine the fracture strength of the granules. The equation described by Adams [64] was considered to determine the fracture strength (τ) of granules, confining the analysis to particles in the range of 850-1180 μm size (preferable size of producing solid oral dosages). Around 0.6 grams of granules were put into a bore die with a diameter of 11.05 mm and the die was then closed with a piston and compressed to a maximum load of 4200 N at a crosshead speed of 3.5 mm/min. The magnesium stearate powders were rubbed on the die surfaces after every three tests to maintain a gentle movement of granules during the fracture strength test. Three repeats were done on the same sample and the error for the estimation of τ was assessed by determining a relative standard error (RSE).

3.6 Genetic Programming Model

A Symbolic Regression (SR) technique was considered for the development of a genetic programming (GP) model. Each GP model (as shown in Figure 3.5) was developed

24

from two inputs such as Reynolds number (Re) and Péclet number (Pe) based on the measured granulation data (from 18 mm and 27 mm twin-screw granulators) to estimate d_{90}, span, and granule fracture strength. Three GP fitting models for the 18 mm extruder and three models for the 27 mm extruder were developed in Python software using the gplearn library. At the first attempt, Shuffle Split cross-validation evaluated the whole granulation dataset during each iteration to generate a training set and a validation set. Two hyper-parameters, such as test_size and train_size regulated the size of the validation and training sets, where the entire dataset was split into 80% of the training set and 20% of the validation set. Ten splitting iterations (n_splits = 10) were set to improve the generalizability of the results, where the training process ensured all the test data was in the design window within the training set. Each GP model was configured based on four functions (log, exp, sin, and cos) and four arithmetic operations (plus, minus, times, and divide) to create simple mathematical equations.
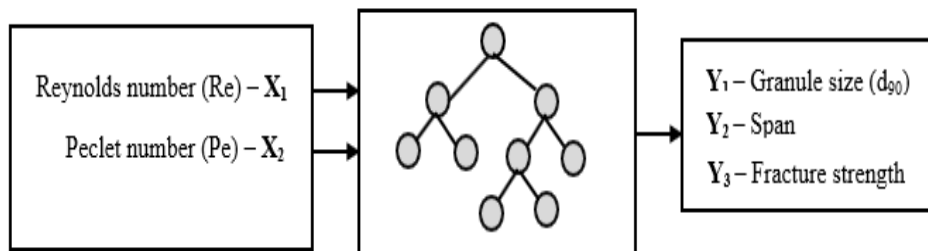
Figure 3.5. GP model for estimating d_{90}, Span, and granule fracture strength.

The efficiency of the GP model was affected by a set of model parameters such as population size, number of generations, tournament size, crossover rate, mutation rate, and reproduction, which combinedly controlled searching for an optimal solution. Table 3.5 lists the selected GP parameters during regression fitting. Artificial intelligence usually demands large datasets, which was not possible in this study; the use of GP modelling in this study is meant for the purpose of proof-of-concept.

Table 3.5 The value of control parameters of GP used in this study.

Parameter	*Set values*
Population size	: 100-250-500
Generations	: 10-20-30
Initialization method	: Grow
Initialization range	: 2-8
Tournament size	: 3-5-7
Crossover rate	: 0.3-0.8
Mutation rate	: 0.05-0.2
Reproduction	: 0.05-0.1
Fitness function	: RMSE
Constant range	: -100 to 100 for d_{90} and -1 to 1 for Span and Fracture strength
Functions & operations	: 'plus', 'minus', 'times', 'divide', 'log', 'exp', 'sin', and 'cos'

CHAPTER 4: RESULTS & DISCUSSION

4.1 Influence of Re and Pe on Mean Residence Time (MRT)
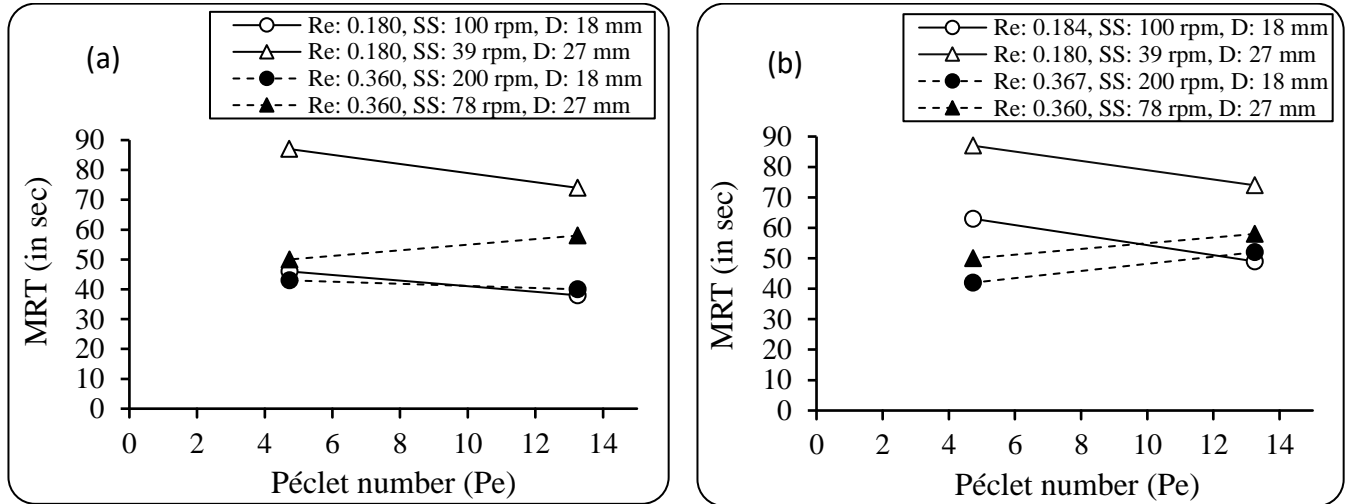
Figure 4.1. Effect of Péclet number (Pe) with varying extruder barrel diameter (D) and Reynolds number (Re) on MRT at (a) L/S ratio = 26% and (b) L/S ratio = 30% [for D = 18 mm with 26% L/S ratio, RSE for MRT = 1.4%, for D = 18 mm with 30% L/S ratio, RSE for MRT = 4.4%, and for D = 27 mm with 26% L/S ratio, RSE for MRT = 5.8%]

Figure 4.1 shows the effect of Péclet number (Pe) on the MRT of the powder inside the barrel when the barrel diameter of the twin-screw extruder was different and Reynolds number (Re) was changed with varying screw speed and liquid fraction (liquid-to-solid ratio) during granulation. The breadth of the residence time distribution (RTD) curves is the extent of how broad or wide the curve is. For both extruders, the MRT of the powder increased because the breadth of the residence time distribution (RTD) curves became narrower for decreasing Pe and rising powder feed rate and liquid fraction (as shown in Appendix Figure A.1, A.2, A.3, and A.4). For both extruders, initially the MRT increased with decreasing Pe (rising powders feed rate) at the low Re and then demonstrated the opposite trend at the higher Re for both liquid fractions (as shown in Figure 4.1 and Appendix Figure A.6). This result agrees with the

27

findings of Dhenge et al. [23], where the authors sharply pointed out that the MRT extended with the powder flow rate and then it reduced for a greater flow rate.

The barrel diameter of twin-screw extruder had a significant effect on the RTD and the MRT of the powder (as shown in Figure 4.1 and Appendix Figure A.5). The analysis of RTD and MRT between the 18 mm and 27 mm extruders revealed that the distribution curves became flattened with powder feed rate, and the powders resided for a longer time inside the barrel of the larger machine because there was a greater free volume inside the machine compared to the smaller extruder. It was also noticed for smaller extruder that rising liquid fraction (from 0.26 to 0.30) increased the Re by reducing wet powder viscosity. It offered additional liquid inside the barrel and increased total amount of material which resulted narrower distribution and higher MRT at smaller Re. The opposite trend was observed at larger Re and this result also agrees with Dhenge et al. [23]. For smaller extruder, changing screw speed (from 100 rpm to 200 rpm) and Re (from 0.180 to 0.360) had the least impact on the RTD and the MRT of the powder. On the other hand, the MRT increased for the larger extruder with accelerating screw speed (from 39 rpm to 78 rpm) because of rising powder feed rate. Hence, it can be stated that the screw speed (and Reynolds number) had the minimum effect on the MRT of the powder for both extruders.

For smaller extruder, the wet granulation experiments were performed with liquid-to-solid ratio of 26% and 30% whereas for larger extruder the experiments were done considering 26% liquid-to-solid ratio. Calculated MRT results from the 18 mm and 27 mm extruders were regressed with both the screw speed (SS) and powders feed rate (PFR) to evaluate their impacts on the MRT. The following equations were established where the values of R^2 were revealed as 0.08, 0.37, and 0.62, respectively:

$$\text{MRT}_{\text{18mm (26\% L/S ratio)}} = -0.02 \text{ (SS)} + 1.3 \text{ (PFR)} + 46.1 \tag{13}$$

$$\text{MRT}_{\text{18mm (30\% L/S ratio)}} = -0.08 \text{ (SS)} - 1.3 \text{ (PFR)} + 65.0 \tag{14}$$

$$\text{MRT}_{\text{27mm (26\% L/S ratio)}} = -0.26 \text{ (SS)} - 1.6 \text{ (PFR)} + 88.1 \tag{15}$$

From the above three equations (Eq. 13 – 15), it was acknowledged that the powder feed rate (and Péclet number) had a greater contribution to the MRT, whereas the screw speed had a much smaller effect on the MRT.

4.2 Estimating Degree of Fill (DF) from Mean Residence Time (MRT)

The degree of fill (DF) is a unique parameter of twin-screw extrusion due to its starved operation, meaning that internal phenomena of mixing and compression for granulation are dependent on the process variables of both feed rate and screw speed. Any differences in behavior between the two extruders were due to their variation in free volume. The free volume inside the barrel of the 27 mm TSE (304 cm^3) was much higher than that of the 18 mm TSE (68 cm^3). The DF was calculated from MRT making the two as correlated descriptors of the process but its dependency on the geometry of the screws also makes it as a more important variable when concerned with scaling.

Calculated DF from the MRT results of 18 mm extruder was regressed with both the SS and PFR to develop statistical models for DF for two liquid fractions (0.26 and 0.30). The regression results showed a strong linear relationship with $R^2 = 0.97$ for the lower liquid fraction and $R^2 = 0.93$ for the higher liquid fraction. The following two expressions were calculated:

$$\text{DF}_{\text{18mm (26\% L/S ratio)}} = -0.01 \text{ (SS)} + 35.5 \text{ (PFR)} + 3.5 \tag{16}$$

$$\text{DF}_{\text{18mm (30\% L/S ratio)}} = -0.11 \text{ (SS)} + 36.3 \text{ (PFR)} + 22.9 \tag{17}$$

Calculated DF from the MRT results of 27 mm extruder was also regressed with both SS and PFR to develop a statistical model for DF for a lower fraction of liquid (0.26). The regression results showed a strong linear relationship with $R^2 = 0.94$. The model was established as:

$$DF_{27mm\ (26\%\ L/S\ ratio)} = -0.07\ (SS) + 9.2\ (PFR) + 8.8 \tag{18}$$

From the three equations (Eq. 16 – 18), it was also obvious that the powder feed rate (and Péclet number) had a more control on the DF compared to the screw speed (and Reynolds number). The DF were predicted from the above three equations and compared with the actual DF (from the measured MRT) to determine the prediction ability (based on R^2) of the three models.

Table 4.1 Predicted and actual DF values for the 18 mm TSE and 27mm TSE

Model	SS (rpm)	Re	PFR (kg/h)	Pe	DF (actual)	DF (predicted)	Error (R^2)
Model 1: $DF_{18mm\ (26\%\ L/S\ ratio)}$	100	0.180	0.5	13.242	15.5	20.1	0.99
	100	0.180	1.4	4.729	52.5	52.0	
	200	0.360	2.2	6.019	75.9	79.2	
	300	0.541	2.4	8.276	86.6	85.1	
Model 2: $DF_{18mm\ (30\%\ L/S\ ratio)}$	100	0.184	1.4	8.276	73.2	63.1	0.95
	200	0.367	1.0	13.242	43	38.0	
	100	0.184	0.5	13.242	20.3	30.4	
Model 3: $DF_{27mm\ (26\%\ L/S\ ratio)}$	39	0.180	0.7	13.242	9.4	12.7	0.97
	78	0.360	3.8	4.729	34.6	38.8	
	117	0.541	2.0	13.242	21.8	19.6	
	117	0.541	5.7	4.729	54.5	53.8	

For smaller extruder, the prediction ability for 26% liquid-to-solid ratio ($R^2 = 0.99$) was very similar to 30% liquid-to-solid ratio ($R^2 = 0.95$). There was no significant difference noticed

between the prediction performance of the 18 mm and 27 mm extruders. For both extruders, the larger variation between the actual and predicted DF was observed at the lower flow rate whereas the smaller deviation between the two DF values was noticed at the higher flow rate of the material.

4.3 Influence of Re and Pe on Degree of Fill (DF)
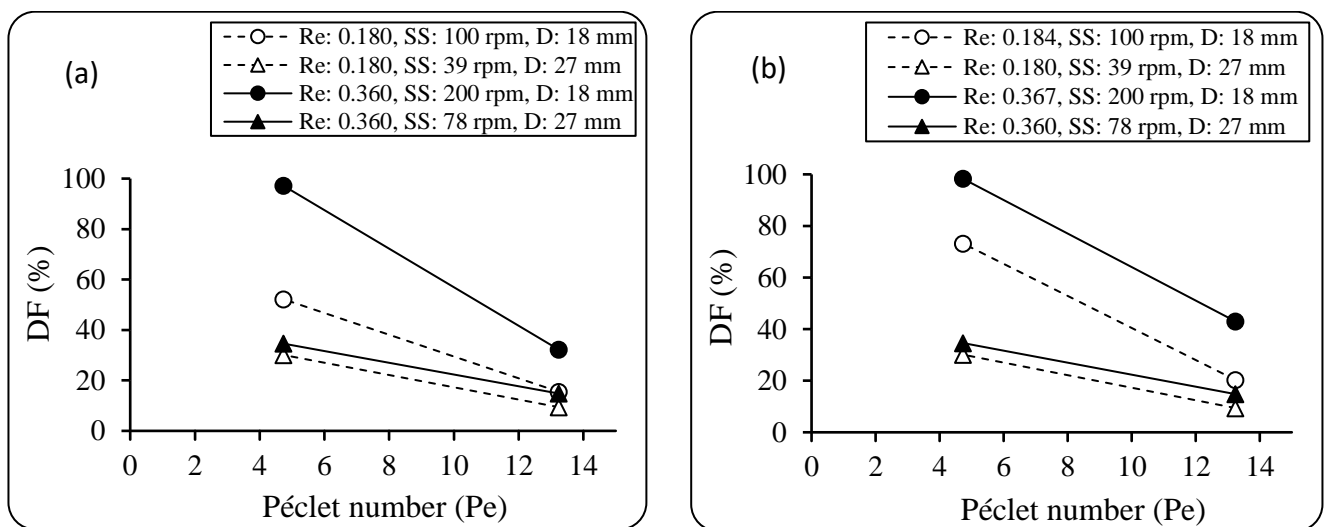
Figure 4.2. Effect of Péclet number (Pe) with varying extruder barrel diameter (D) and Reynolds number (Re) on DF at (a) L/S ratio = 26% and (b) L/S ratio = 30% [for D = 18 mm with 26% L/S ratio, RSE for DF = 8.3%, for D = 18 mm with 30% L/S ratio, RSE = 17.1%, and for D = 27 mm with 26% L/S ratio, RSE = 6.6%]

Figure 4.2 shows the influence of Péclet number (Pe) on DF inside the barrel when the barrel diameter of the extruder was different and Reynolds number (Re) varied (because of increased screw speed and higher liquid fraction). It was observed for all extruders that the DF increased significantly with decreasing Pe and increase of powder feed rate. For smaller extruder, the increase in DF with powder feed rate was more obvious compared to the larger extruder because of difference in free volume inside the two extruders. The same trend was noticed for all Re when the feed rate of the powder was increased (as shown in Figure 4.2(a)). Under a specific powder flow rate, the conveying capacity of the screws usually improve

because of increasing screw speed, which reduces the DF inside the barrel. In this study, increasing Re (from 0.180 to 0.360) or accelerating screw speed (from 100 rpm to 200 rpm) increased the DF because of rising total flow rate inside the extruders (as shown in Figure 4.2(a)). Hence, it can be stated that the screw speed or the Re had the least effect on the DF. For 18 mm extruder, rising liquid fraction (from 0.26 to 0.30) increased the Re by reducing wet powder viscosity. The DF also raised up with the liquid fraction, as there was additional liquid inside the barrel which increased the total material flow rate during granulation process (as shown in Figure 4.2(b)). A significant impact of DF on the PSD and granule fracture strength has been revealed and described in the next section.

4.4 Influence of Re and Pe on d_{90} and Span of PSD
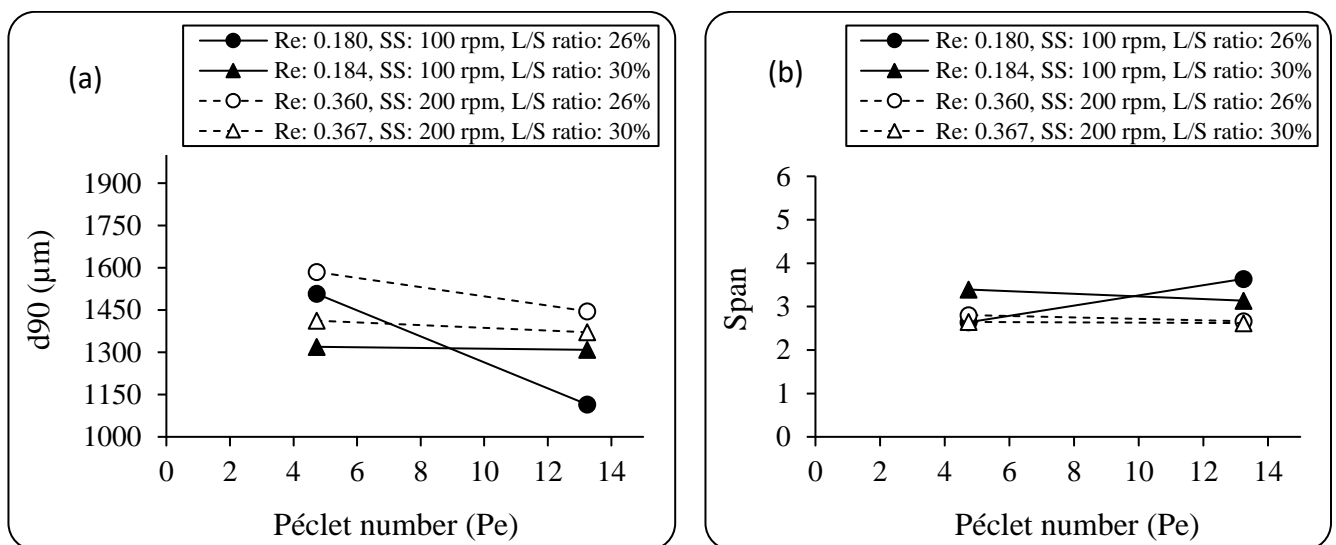
Figure 4.3. Effect of Péclet number (Pe) with varying L/S ratio (%) and Reynolds number (Re) on (a) d_{90} and (b) Span [for D = 18 mm with 26% L/S ratio, RSE for d_{90} & Span =46% & 0.2% and D = 18 mm with 30% L/S ratio, RSE for d_{90} & Span =24% & 0.2%]

Figure 4.3 shows the effect of Péclet number (Pe) on d_{90} and span while the fraction of liquid and Reynolds number differed for wet granulation in the 18 mm extruder. For all powder feed rates, the distributions of granule size were bimodal (as shown in Appendix Figure A.7),

which included the presence of a high percentage of both small- and large-size granules. According to Dhenge et al. [23] and Osorio et al. [1], the bimodal distribution can be changed to monomodal with increasing liquid fraction, though only bimodal distributions were observed in this study for the two liquid fractions considered (as shown in Appendix Figure A.10); the increase in liquid fraction from 0.26 to 0.30 was not adequate to reach the monomodal distribution. For smaller extruder, the increase in powder feed rate (from 0.5 kg/h to 2.8 kg/h) and decrease of Pe (from 13.242 to 4.729) reduced the proportion of fines and increased the proportion of large granules for both liquid fractions (as shown in Appendix Figure A.10). This result agrees with Osorio et al. [1].

It was also noticed in the figure that the d_{90} increased with a decrease in Pe or an increase in powder feed rate for either liquid fraction studied (as shown in Figure 4.3(a)). The powder feed rate largely determined the degree of fill inside the twin-screw extruder, with increasing fill leading to greater compaction of the powders and hence, rise in d_{90}. This result agrees with the result of Djuric et al. [16]. Shifting screw speed (from 100 rpm to 200 rpm) also increased the d_{90} along with the total feed rate, though it had a much smaller effect on the wet granulation process. Besides, the d_{90} reduced with an increase in the fraction of liquid and it agrees with the result of Dhenge et al. [23]. The exception was only observed for lower Re at higher Pe, where rising the liquid fraction (from 0.26 to 0.30) increased the value of d_{90} and it agrees with Osorio et al. [1].

For lower fraction of liquid, the span of PSD decreased from 3.6 to 2.6 with powder feed rate at smaller Re, whereas no change in the span was observed at larger Re. Besides, for the higher liquid fraction, there were no significant changes in the span of PSD (as shown in Figure 4.3(b) and Appendix Figure A.12). In other words, the span of PSD was consistent for

both liquid fractions when the Re was higher, though a reason for the deviation in span for smaller Re at the lower liquid fraction could not be found.
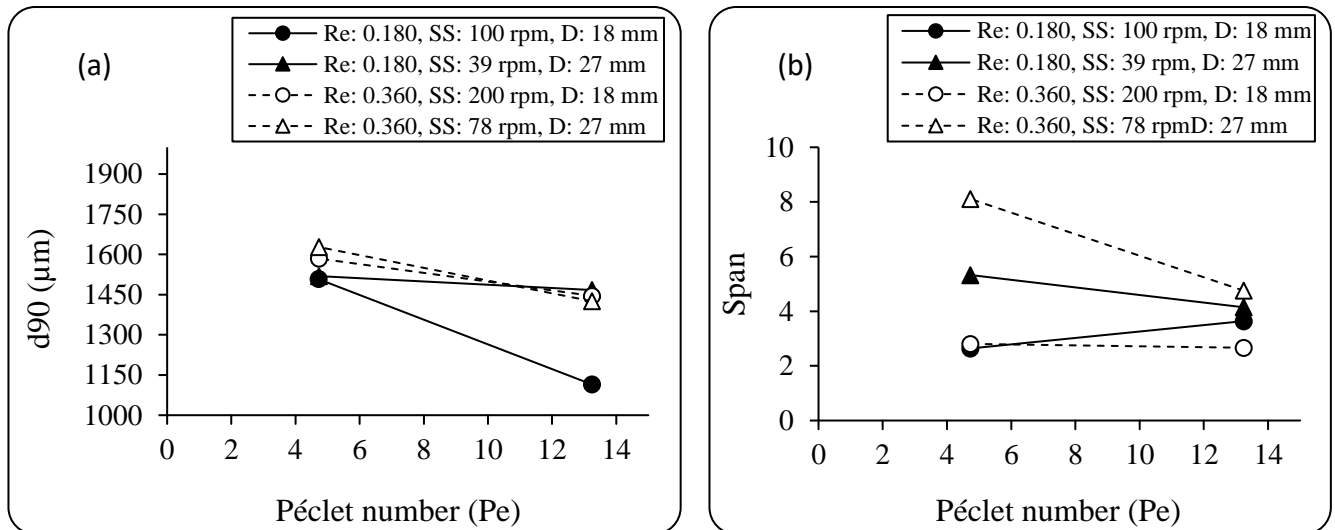

Figure 4.4. Effect of Péclet number (Pe) with varying extruder barrel diameter (D) and Reynolds number (Re) on (a) d_{90} and (b) Span (for 26% L/S ratio) [for D = 27 mm, RSE for d_{90} & Span =28% & 0.6%]

Figure 4.4 shows the effect of Péclet number (Pe) on the d_{90} and span of PSD when the Reynolds number (Re) were varied during wet granulation in the larger extruder. For 27 mm extruder, both the percentage of fines and large granules increased with powder feed rate. Rising powder feed rate (from 0.7 kg/h to 3.8 kg/h) and decreasing Pe (from 13.242 to 4.729) produced granules with broader distribution (as shown in Appendix Figure A.9). Comparing the two extruders demonstrated that a higher percentage of fines was obtained for the small-scale extruder (as shown in Appendix Figure A.11). A reason for this could be a small gap (0.3-0.7 mm) between the surfaces of inner barrel and screw in the 18 mm extruder which led to more efficient breakage and produced a greater proportion of fines. For the selected formulation, the d_{90} was significantly affected by the powder flow rate compared to other moments of the PSD. The same formulation was granulated on both extruders, although the extruder scale had a meaningful impact on the granule properties. The granules produced by

the 27 mm extruder were coarser than the 18 mm extruder (as shown in Figure 4.4(a)). The barrel diameter and the size of the granule (d_{90}) increased almost linearly. For larger extruder, a higher consolidation rate and more liquid saturation during granulation could be a reason for the increase of d_{90}. This result also agrees with the findings of Djuric et al. [16] and Osorio et al. [1]. Rising powder feed rate increased in the proportion of large-size granules for the 27 mm extruder, as the greater DF in the extruder barrel caused more densification.

For larger extruder, the span of PSD significantly increased because of rising the granule size (d_{90}) compared to the smaller extruder (as shown in Figure 4.4(b) and Appendix Figure A.13). The variations in the consolidation and agglomeration behavior between the two extruders could make these differences in the granule size and span of PSD.

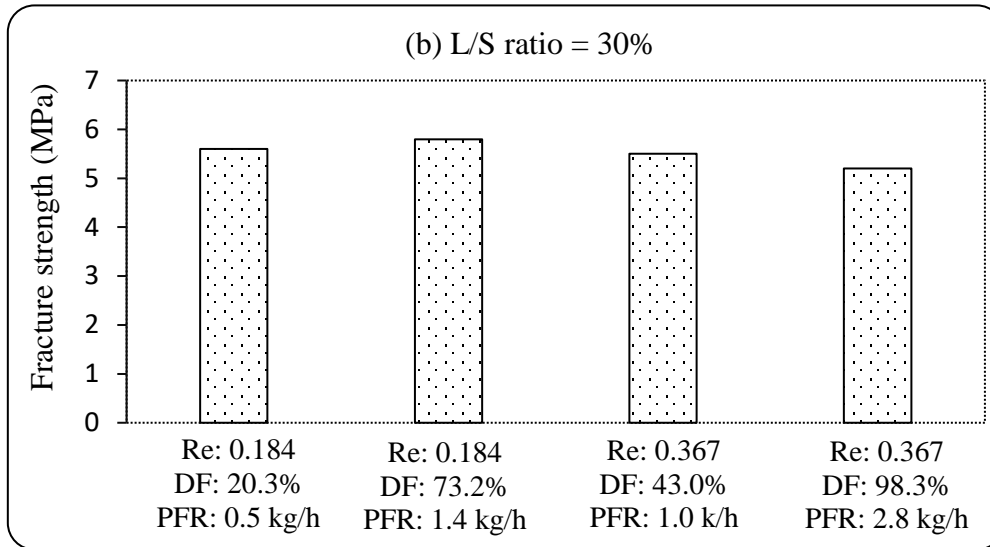## 4.5 Influence of Re and Pe on Fracture Strength of Granules
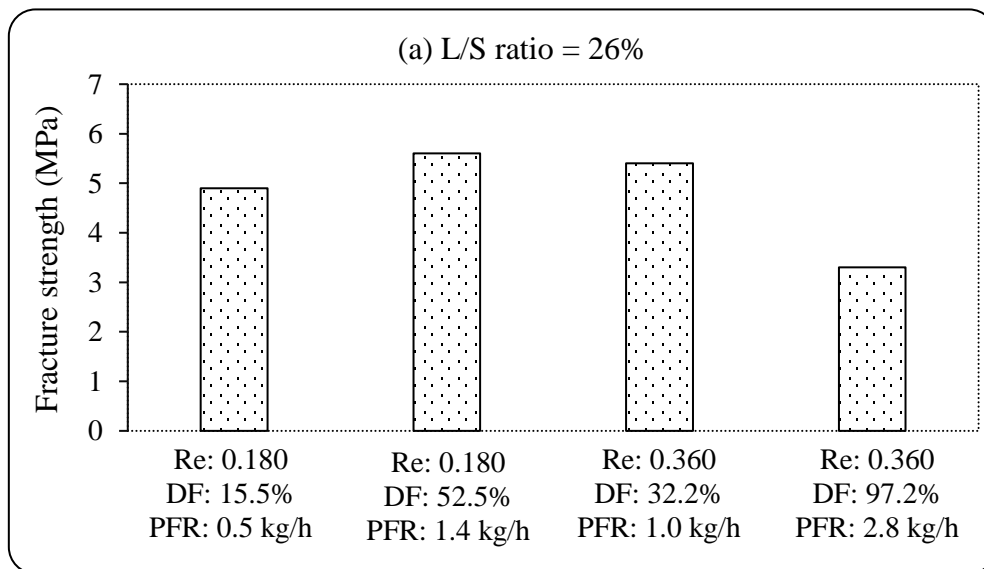
Figure 4.5. Effect of Degree of fill (DF) and Reynolds number (Re) on Fracture strength (FS) with D = 18 mm at (a) L/S ratio = 26% and L/S ratio = 30% [for 26% L/S ratio, RSE for FS = 0.4% and for 30% L/S ratio, RSE for FS = 0.1%]

Figure 4.5 demonstrates the effect of DF and Re on granule fracture strength when wet granulation was performed with different fractions of liquid in the 18 mm extruder. For lower liquid fraction, the fracture strength of granules at smaller Re (100 rpm screw speed) increased with the DF because of increased capillary action in the presence of many powdered particles. At the larger Re (screw speed of 200 rpm), the fracture strength of granules reduced with increasing DF because there might have lower capillary saturation to form stronger granules. On the other hand, a higher liquid fraction decreased the apparent viscosity of the wet powders which increased Re and improved the fracture strength for all conditions. A reason for this could be the slurry saturation for added liquid which led to interlocking many of the primary (fine) particles together and thus produced stronger granules. This result also agrees with the findings of both Osorio et al. [1] and Dhenge et al. [23].
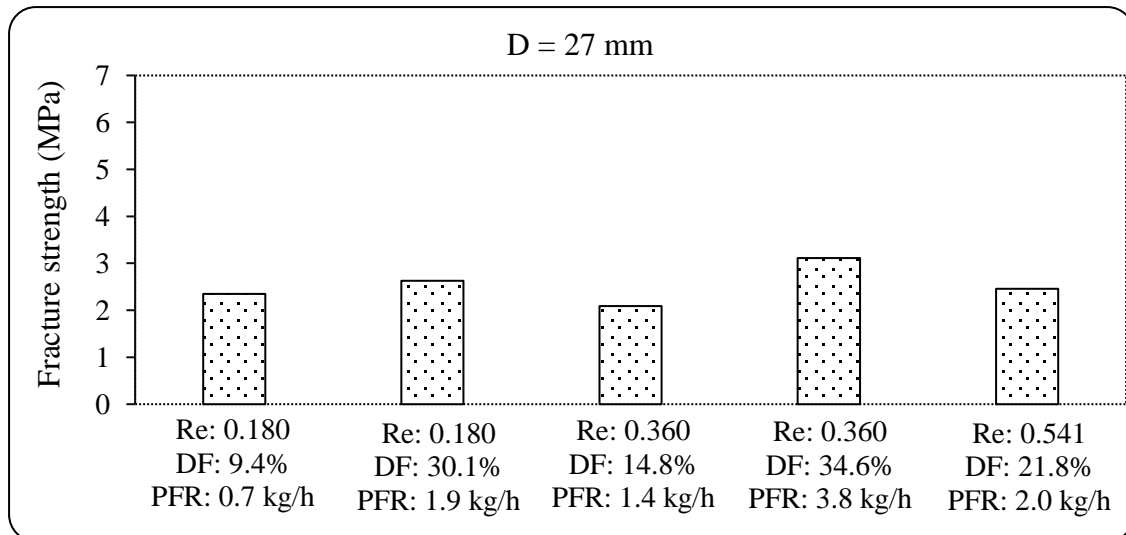
Figure 4.6. Effect of Degree of fill (DF) and Reynolds number (Re) on Fracture strength (FS) with L/S ratio = 26% at D = 27 mm [for D = 27 mm, RSE for FS= 0.2%]

Figure 4.6 shows the effect of DF and Re on granule fracture strength with lower liquid fraction when the wet granulation experiments were performed in the 27 mm twin-screw extruder. The increasing strength of the granules was caused by the increasing DF at higher powder feed rates. For smaller extruder, the granule fracture strength increased with DF at smaller Re, though the strength decreased with a further increase of DF at higher Re. Besides, the fracture strength increased with DF for all Re for the larger extruder. The fracture strength of granules produced from the two extruders were not the same, as the free volume inside the extruder barrel and compaction of the powders were different. Smaller extruder produced stronger granules whereas the larger extruder formed granules with poor strength.
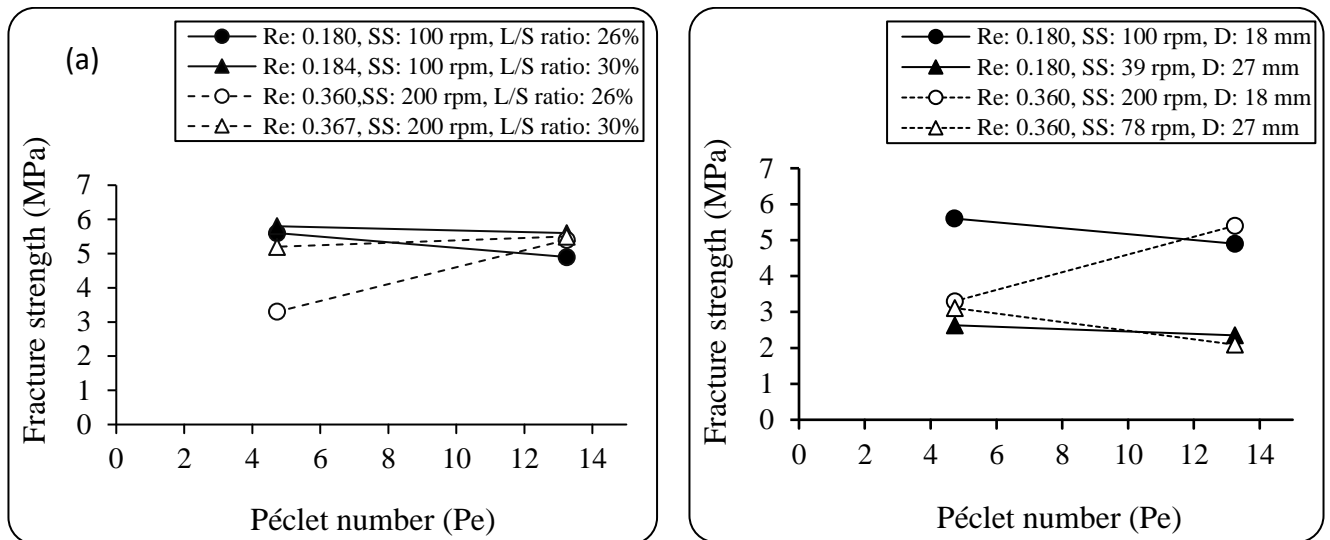
Figure 4.7. Effect of Péclet number (Pe) with varying (a) L/S ratio (%) and (b) extruder barrel diameter (D) on Fracture strength (FS) [for D = 18 mm with 26% L/S ratio, RSE for FS = 0.4%, for D = 18 mm with 30% L/S ratio, RSE for FS = 0.1%, and for D = 27 mm with 26% L/S ratio, RSE for FS = 0.2%]

Figure 4.7 shows the effect of Péclet number (Pe) on granule fracture strength with varying liquid fraction and extruder barrel diameter. The fracture strength of the granules increased for decreasing Pe (from 13.242 to 4.729) and rising powder feed rate. For both extruders, higher powder feed rate compacted the powders inside the extruder barrel and formed stronger granules. This result agrees with Fu et al. [65], who noticed in a batch high-shear mixer that if granulations are done for a long time, the strength still increases. The compaction of the powder was higher inside the barrel of 18 mm extruder, which produced stronger granules compared to the larger extruder. This result also agrees with the findings of Dhenge et al. [23]. It is obvious that the powder feed rate (and Péclet number), Reynolds number, degree of fill, liquid-to-solid ratio, and scales of the twin-screw extruder had significant control on the fracture strength of granules.

4.6 Establishing Scaling-Up Rules for TSWG

4.6.1 Results of GP

This project involved use of a GP based Symbolic regression optimized tool to develop the following three fitting equations with associated tree diagrams (as shown in Appendix Figure A.14) for the 18 mm twin-screw extruder to estimate d_{90}, span of PSD, and fracture strength (FS) of granules, where the correlation coefficient R-squared (R^2) values calculated from the GP fitting process were reflected as $0.23, 0.11$, and 0.55, respectively:

$$d_{90(18mm)} = 0.6 * Re^2 - (Re + 26.7)(Pe - 57.3) + \log_{10}(69 * Re) + 61.6 \tag{19}$$

$$Span_{(18mm)} = 2 * Re + \sin(Re + 0.9) + \sin(2 * Re - \sin(\cos(Pe + \cos(Re))) + 0.9) + 0.9 \tag{20}$$

$$FS_{(18mm)} = -\log_{10}(Re) + \log_{10}(Pe) + \log_{10}(e^{Pe} - \log_{10}(Re) + \log_{10}(Pe)) \tag{21}$$

GP also developed the following three fitting equations with related tree diagrams (as shown in Appendix Figure A.15) for 27 mm extruder to predict d_{90}, span of PSD, and granule fracture strength (FS), where R^2 values were observed as $0.60, 0.98$, and 0.63, correspondingly:

$$d_{90(27mm)} = Pe^2 + (Re + 26.3)(-Re + e^{Re} + 48.8) + e^{Re} \tag{22}$$

$$Span_{(27mm)} = \cos(Re) + \cos(Re^2) + \cos(\cos(-Re + Pe + \sin(\sin(Pe^2)))) + 2.4 \tag{23}$$

$$FS_{(27mm)} = 0.3 * Re - \log_{10}\left(\log_{10}(0.5 * e^{Pe} + 0.8)\right) + 2.7 \tag{24}$$

By selecting appropriate values of control parameters and based on the root mean squared error (RMSE) as fitness function, GP generated the above six optimal mathematical expressions for both small and large extruder. The model which offered the lowest RMSE, and the highest R^2 values was chosen as the best model in each case. All GP-derived equations (Eq. 19 – 24) exhibited a nonlinear nature between the dependent variables (d_{90}, span & fracture strength) and the independent variables (Re and Pe). It was observed from Eq. (19) that the Re

had a larger positive effect and the Pe had a negative effect on the granule size (d_{90}) for the smaller extruder. For larger extruder, the Eq. (22) revealed that the Pe now influenced the d_{90} more than the Re. Considering the span of PSD, there was a considerable positive effect of Re on the breadth of PSD in the smaller extruder (Eq. 20). For larger extruder, the Re and Pe positively impacted the span value (Eq. 23). Finally, from Eq. (21) and Eq. (24), it was realized for the smaller extruder that the Re had a negative effect, but the Pe had a positive effect on the fracture strength of granules whereas the Pe had a negative effect but the Re had a positive effect for the larger extruder.

By comparing between the two equations of d_{90} (Eq. 19 & Eq. 22), it was observed that both the equations were simpler (in regard to number of terms and the implied non-linearity of those terms). For the larger extruder, the predictive performance of the model was better ($R^2 =$ 0.60) indicating good representation of the relationship between the upper moment of the PSD (d_{90}) and the two dimensionless numbers when compared to the smaller extruder ($R^2 = 0.23$); this was likely due to the greater sensitivity of d_{90} to operating variables in the 27 mm TSE, making one specific arrangement of expressions in the equation for GP more apparent. The two equations for span of PSD (Eq. 20 & Eq. 23) were simpler, though the fit of the equation for the larger extruder was better ($R^2 = 0.98$) than for the smaller extruder ($R^2 = 0.11$). The equations of granule fracture strength for small-size and large-size extruders (Eq. 21 & Eq. 24) were also simpler though the fit of the equation for the larger extruder was better ($R^2 = 0.63$) when compared to the smaller extruder ($R^2 = 0.55$).
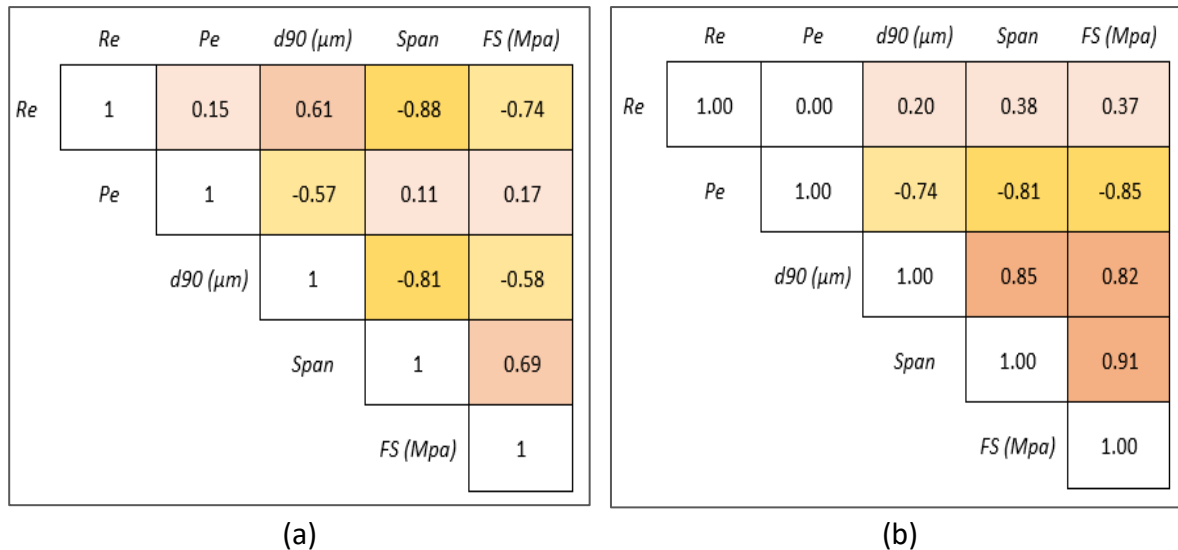
	Re	Pe	d90 (μm)	Span	FS (Mpa)
Re	1	0.15	0.61	-0.88	-0.74
Pe		1	-0.57	0.11	0.17
d90 (μm)			1	-0.81	-0.58
Span				1	0.69
FS (Mpa)					1

(a)

	Re	Pe	d90 (μm)	Span	FS (Mpa)
Re	1.00	0.00	0.20	0.38	0.37
Pe		1.00	-0.74	-0.81	-0.85
d90 (μm)			1.00	0.85	0.82
Span				1.00	0.91
FS (Mpa)					1.00

(b)

Figure 4.8. Interaction between input parameters based on Pearson correlation for (a) D = 18 mm and (b) D = 27 mm.

All GP-derived mathematical equations (Eq. 19 – 24) showed moderate to strong correlations between the examined dimensionless independent variables (Re and Pe) and dependent variables (d_{90}, Span, and granule fracture strength). The correlation analysis (as shown in Figure 4.8) showed that the Re had a greater influence on d_{90}, span, and fracture strength for smaller extruder (D = 18 mm) when compared to the larger extruder (D = 27 mm). On the contrary, Pe had a larger impact on the d_{90}, span, and fracture strength of granules for the 27 mm extruder.

Two dimensionless numbers including Re and Pe were fixed in this study to scale up the wet granulation system from 18 mm to 27 mm extruder. For smaller extruder, the Re (0.180, 0.360, and 0.541) calculated based on varying screw speed (100 rpm, 200 rpm, and 300 rpm) were constant for the larger extruder to examine the scalability of TSWG on the machine. The Pe (13.242, 8.276, 6.019, and 4.729) calculated based on changing material flow rate under a fixed screw speed was constant to determine new powder flow rates for different screw speeds. The correlation analysis revealed that the DF was greatly influenced by the Péclet number (and

powder feed rate), Reynolds number (and screw speed), and the scale of the two extruders. The following statistical regression equations were found for this relationship between DF and the operating factors of Re and Pe, with R^2 values observed as 0.92 and 0.94, respectively:

$$DF_{18 \text{ mm}} = 133.5 \text{ (Re)} - 6.1 \text{ (Pe)} + 67.8 \qquad (25)$$

$$DF_{27 \text{ mm}} = 51.0 \text{ (Re)} - 2.9 \text{ (Pe)} + 34.9 \qquad (26)$$

For small-size extruder, there was fairly positive correlation (0.50) between the Re and the DF whereas the Pe had a strong negative correlation (-0.62) with the DF. For large-size extruder, the Re had a moderate positive correlation (0.51) with the DF and the Pe had a very strong negative correlation (-0.83) with the DF. This means, the DF inside the extruder barrel increased with the Re but significantly decreased with the Pe for reducing powder flow rate which greatly impacted the granulation properties (d_{90}, span, and fracture strength) on the small- and large-size machines.

Sensitivity analysis was performed to understand the functional relationship between each of the independent factors (Re and Pe) and the dependent factors (d_{90}, span, and fracture strength); testing for sensitivity indicates which dimensionless number and its related operational variables mattered the most to the granulated product. A realistic evaluation range for Re (0.09 – 0.54) and Pe (7.4 – 13.0) was identified based on the calculation of degree of fill (when DF values were positive and not exceeding 100%) for both extruders using Eq. 25 and 26.

The contour plots shown in Figures 4.9 – 4.11 are given to demonstrate the sensitivities of the GP-derived equations as Re and Pe were altered within their stated limits for the two extruders.
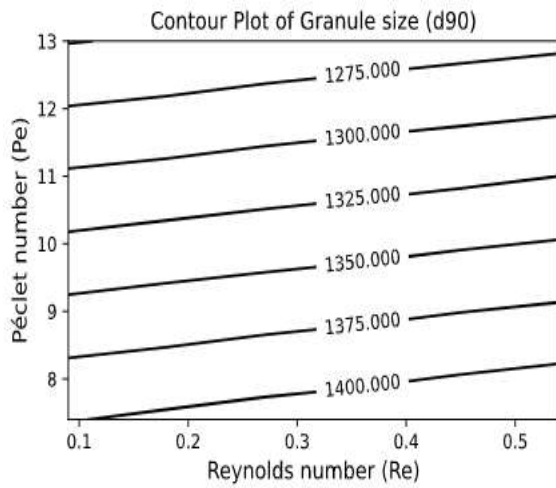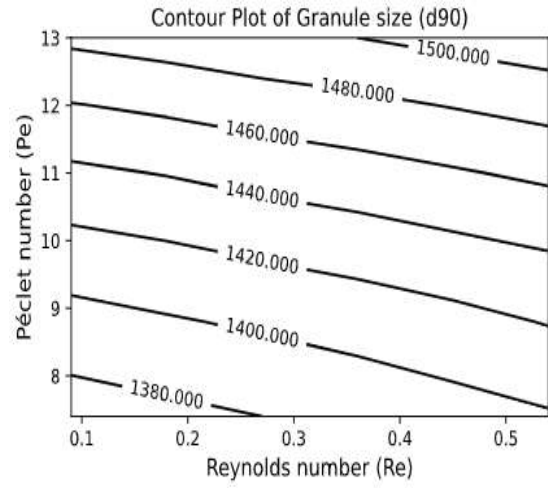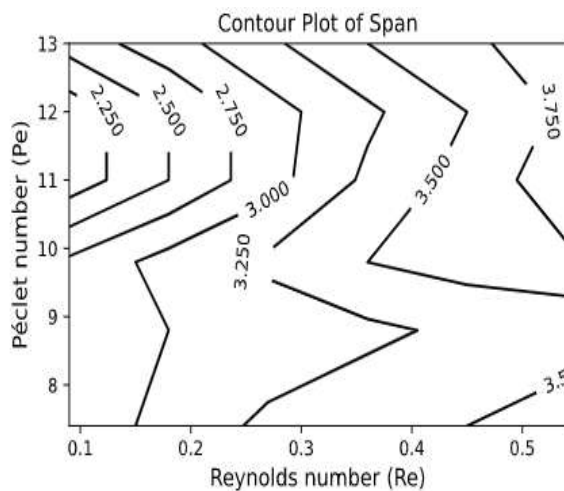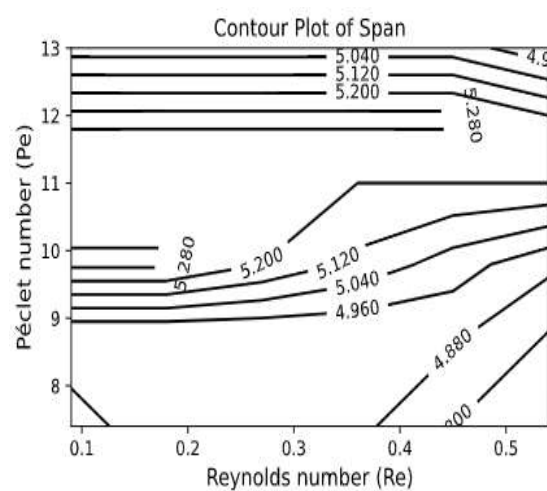
Figure 4.9. Contour plots of Granule size (d_{90}) versus the Re and Pe for (a) 18 mm TSE and (b) 27 mm TSE on the basis of regression equations generated via Genetic programming.

Figure 4.9 demonstrates the contour plots of granule size (d_{90}) for the 18 mm and 27 mm twin-screw extruders where the plots of d_{90} revealed strong linear behavior in both cases. It was observed that both Pe and Re contributed equally to the larger granule sizes, denoted by d_{90}, though their influence was completely opposite one another between the two machines. Increasing Re had a positive effect in the 18 mm extruder and a negative effect in the 27 mm extruder. Conversely, increasing Pe had a negative effect in the 18 mm extruder and a positive effect in the 27 mm extruder.

Figure 4.10. Contour plots of Span of PSD versus the Re and Pe for (a) 18 mm TSE and (b) 27 mm TSE on the basis of regression equations generated via Genetic programming.

Figure 4.10 illustrates the contour plots of span for the small and large twin-screw extruders as Re and Pe were tested over their stated ranges. It was noticed that the span was much more sensitive to Re compared to Pe in the 18 mm extruder and in the case of the 27 mm extruder, span was close to being completely insensitive to Re.
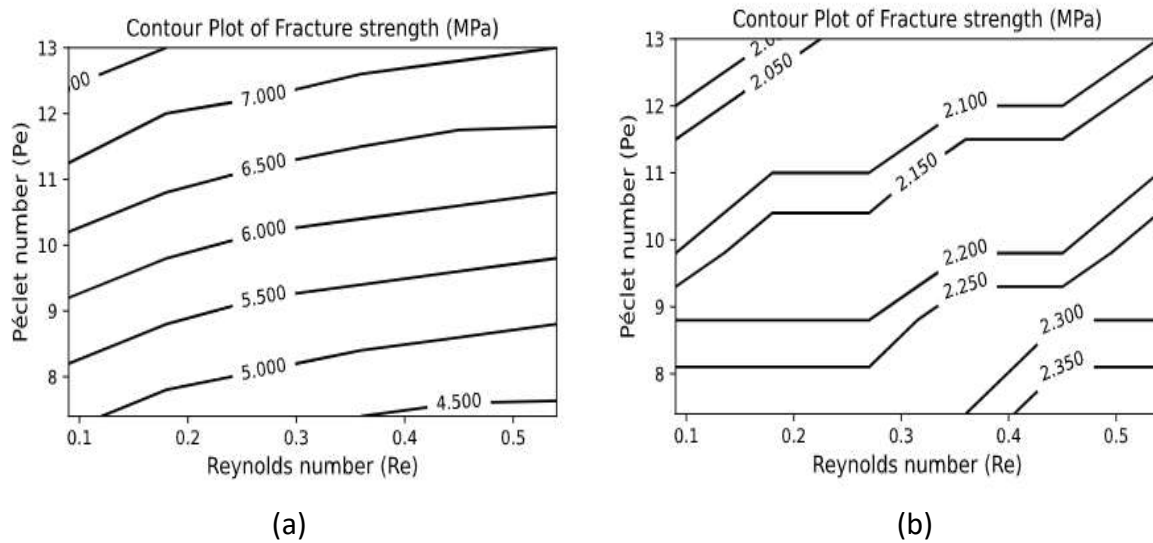

(a)   (b)

Figure 4.11. Contour plots of fracture strength versus the Re and Pe for (a) 18 mm TSE and (b) 27 mm TSE on the basis of regression equations generated via Genetic programming.

Finally, Figure 4.11 demonstrates the contour plots of granule fracture strength for small- and large-size extruders when Re and Pe were tested over their stated ranges. For the larger extruder, both Re and Pe influenced fracture strength of the granule. As expected, the influence of changing Re and Pe on increasing fracture strength correspondingly produced small d_{90} values in this machine. In the 18 mm extruder, Pe had a significant effect on fracture strength, and the same was true for Re but only at low values; for Re of 0.4 and above, fracture strength showed diminishing sensitivity to this dimensionless number.

With sensitivity of the dimensionless numbers established above, we now examine the reasonableness of predictions by the six GP fitting equations using experimental data, as listed in Table 4.2 and Table 4.3.

Table 4.2 External validation set for the 18 mm TSE to test the predictive ability of GP.

Factor		Observed value			Predicted value		
Re	Pe	d_{90} (μm)	Span	Fracture strength (MPa)	d_{90} (μm)	Span	Fracture strength (MPa)
0.345	6.389	1675	3.4	3.4	1440	3.3	4.0
0.345	4.259	2100	4.9	4.3	1498	3.4	2.9
0.517	9.583	1550	3.4	6.5	1362	3.6	5.4
0.517	6.389	1975	5.3	3.4	1449	3.8	3.9

Table 4.3 External validation set for the 27 mm TSE to test the predictive ability of GP.

Factor		Observed value			Predicted value		
Re	Pe	d_{90} (μm)	Span	Fracture strength (MPa)	d_{90} (μm)	Span	Fracture strength (MPa)
0.718	12.103	1375	3.6	0.9	1503	4.6	2.2
0.718	6.051	1300	4.3	3.8	1393	5.0	2.5
1.080	13.643	1600	3.0	2.1	1577	4.0	2.3
1.080	6.822	1350	3.8	2.7	1437	3.8	2.6

***External dataset (observed values) for validation in the tables above were collected from the M.ASc. Thesis of Zequn Shi (September 2022), Department of Chemical Engineering, McMaster University.

The following six plots demonstrated the observed versus predicted values for the above six fitting equations based on whole data set.
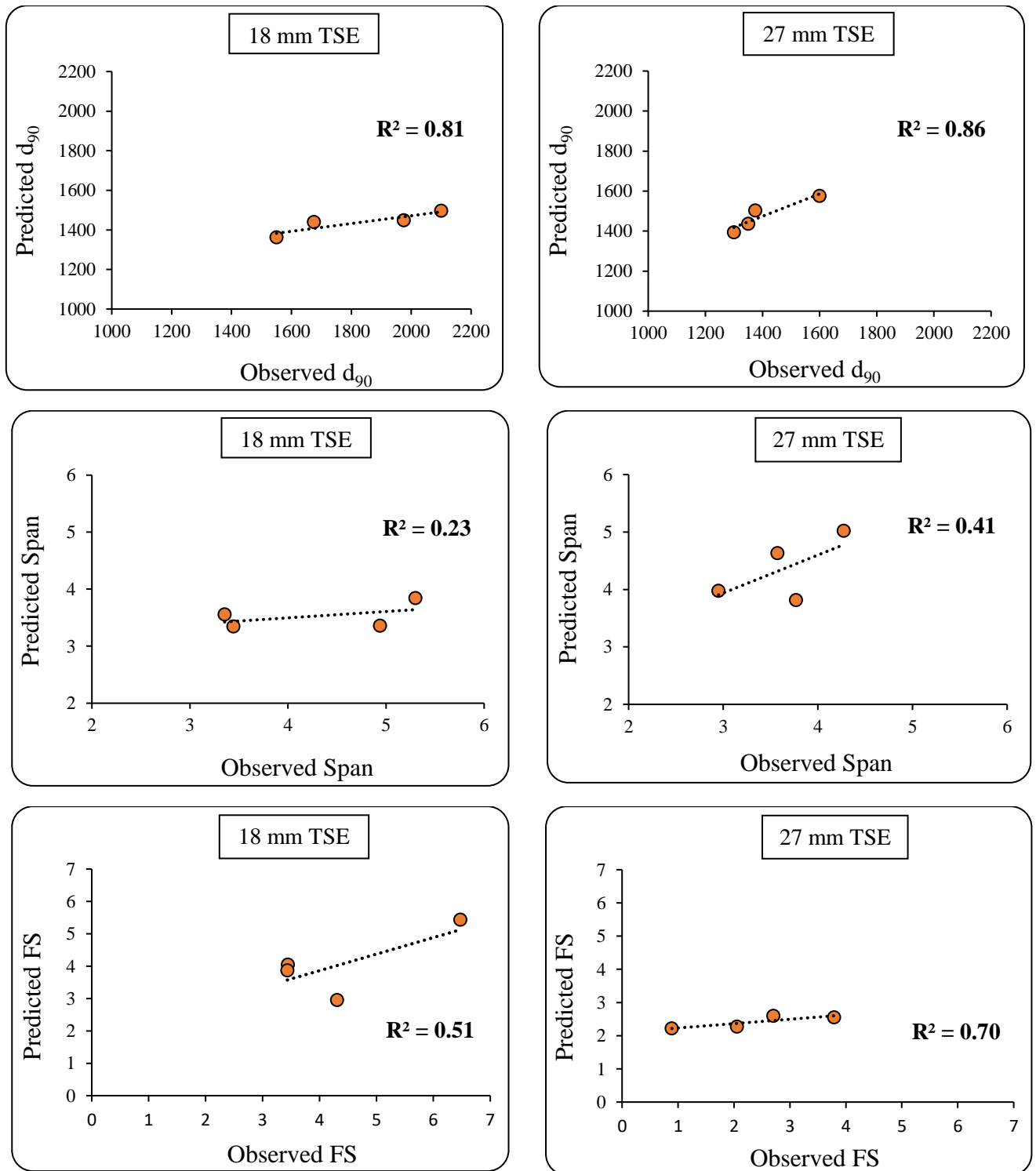
Figure 4.12. Scatter plots of observed versus predicted d_{90}, Span, and Fracture strength (FS) of granules by the GP models for 18 mm TSE and 27 mm TSE. Line included for clarity.

Figure 4.12 shows the scatter plots and R^2 values for the four sets of conditions (as shown in Tables 4.2 & 4.3) with the two extruders. Data lining up along a 45-degree line

projecting from the origin in each plot would reveal a perfect fit. It was noticed in the small-size extruder that the fit for the granule fracture strength was better than the d_{90} and span of PSD. In the large-size extruder, the fits for the d_{90} and span were better than the fracture strength of granules. The size of the error for the d_{90} in the 18 mm and 27 mm extruders were almost similar ($R^2 = 0.81$ & 0.86) as the d_{90} in the two machines had the same sensitivity to the dimensionless numbers (Re and Pe). The error size for the span in the smaller extruder ($R^2 = 0.23$) was more than the error size in the larger extruder ($R^2 = 0.41$). The reason for this could be the span that was sensitive to Re but mostly insensitive to Pe in the 18 mm machine although in the 27 mm it was insensitive to both of the dimensionless parameters. This means, the effect of Re on the span in the 18 mm extruder was more than the Pe which led to more changes in the predicted values of span when the Re was varied and resulted larger error when compared to the 27 mm extruder. The size of the error for the granule strength in the larger extruder ($R^2 = 0.70$) was lower than the error size in the smaller extruder ($R^2 = 0.51$). The reason for this could be the strength of the granule which was sensitive to Pe but insensitive to Re in the 27 mm extruder where it was mostly sensitive to Pe compared to the Re in the 18 mm extruder. The influence of Pe on the granule strength in the 18 mm extruder was higher than the Re which led to drastic changes in the predicted values of strength when the Pe was varied and caused greater error as compared to the 27 mm extruder. Overall, the fits for the granule properties in the two extruders were appeared to be moderate above and the error size in the two machines were varied because of unusual sensitivity of the GP equations to the dimensionless numbers. The predictability of the GP was also less because of using limited data for GP modelling.

4.6.2 Proposed Scaling Rules

The fitted equations stipulated above can be potentially employed to formulate granules under the general viewpoint of QbD product development. It will also help to create a standard processing window to identify a suitable product design space and control the approach. The following scaling rules have been established from the Eq. 19 – 24:

$$\frac{D_{18mm}}{D_{27mm}} = \frac{D_{90(18mm)}}{D_{90(27mm)}} = \frac{0.6*Re^2-(Re+26.7)(Pe-57.3)+\log_{10}(69*Re)+61.6}{Pe^2+(Re+26.3)(-Re+e^{Re}+48.8)+e^{Re}} \tag{27}$$

$$\frac{D_{18mm}}{D_{27mm}} = \frac{Span_{(18mm)}}{Span_{(27mm)}} = \frac{2*Re+\sin(Re+0.9)+\sin(2*Re-\sin(\cos(Pe+\cos(Re)))+0.9)+0.9}{\cos(Re)+\cos(Re^2)+\cos(\cos(-Re+Pe+\sin(\sin(Pe^2))))+2.4} \tag{28}$$

$$\frac{D_{18mm}}{D_{27mm}} = \frac{FS_{(18mm)}}{FS_{(27mm)}} = \frac{-\log_{10}(Re)+\log_{10}(Pe)+\log_{10}(e^{Pe}-\log_{10}(Re)+\log_{10}(Pe))}{0.3*Re-\log_{10}(\log_{10}(0.5*e^{Pe}+0.8))+2.7} \tag{29}$$

Beside the Re and Pe, the DF was identified as an important aspect of granulation in this study, though it was not fixed unlike Re and Pe. For an efficient scale-up on the twin-screw extruder, it now seems likely that the DF should be considered as another dimensionless number that should be constant between the two sizes of extruders being scaled. The following table (Table 4.4) considered the identical DF for the two twin-screw extruders to examine the scalability of TSWG on the machine and understand the effect of scaling on the granule properties (d_{90} span and granule fracture strength). The values of Re and Pe were determined from the Eq. 25 & Eq. 26 and the d_{90}, span and fracture strength were predicted from the Eq. 27 – 29.

Table 4.4 Effect of scaling on the d_{90}, span and granule fracture strength

DF (%)	Re	Pe	D_{90} (µm) (Predicted)	Span (Predicted)	Fracture strength (MPa) (Predicted)

		18 mm TSE	27 mm TSE	18 mm TSE	27 mm TSE	18 mm TSE	27 mm TSE	18 mm TSE	27 mm TSE
5	0.10	12.48	12.07	1264	1462	2.4	5.0	7.5	5.8
10	0.20	13.85	12.10	1232	1468	3.1	4.9	7.9	6.2
25	0.35	14.68	9.57	1216	1422	3.2	5.0	8.0	6.5
40	0.45	14.41	6.16	1228	1375	3.3	4.9	7.8	6.6
50	0.50	13.86	3.59	1245	1353	3.5	4.8	7.5	6.8
60	0.65	15.50	2.78	1207	1359	3.4	4.7	8.1	7.4
75	0.80	16.33	0.24	1190	1363	3.9	4.5	8.4	8.4

The following three plots exhibited the effect of scaling on the granule properties when the DF was assumed constant in the 18 mm and 27 mm twin-screw extruders.
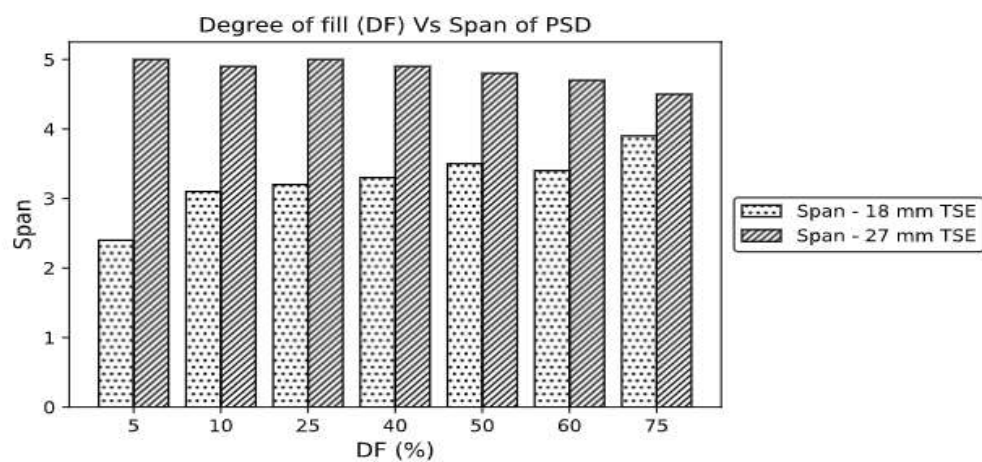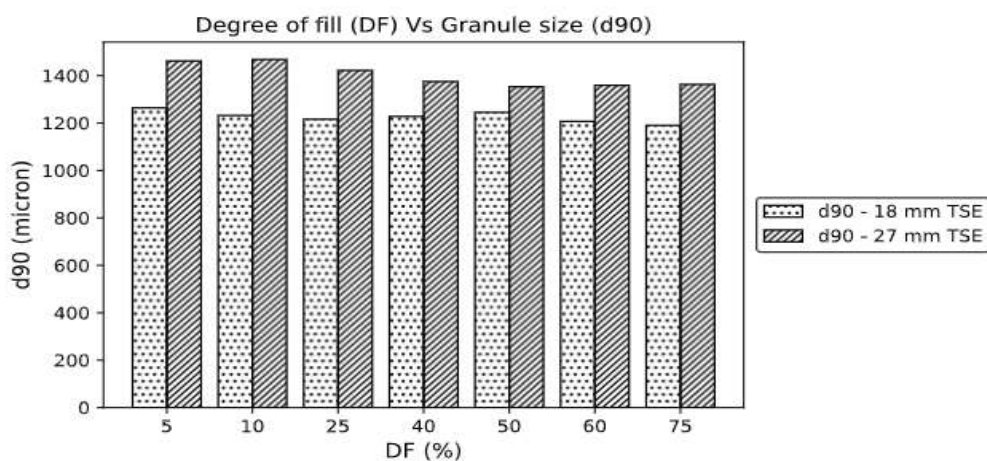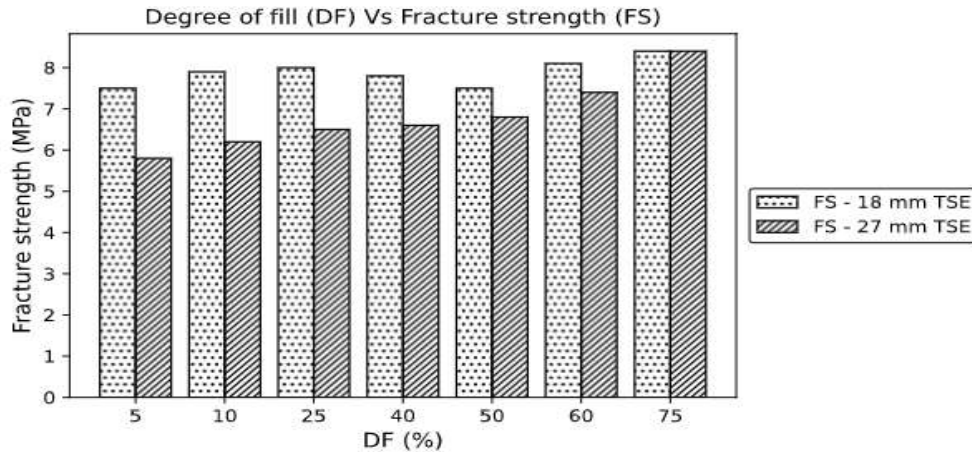
Figure 4.13. Bar charts of DF versus Granule properties for 18 mm TSE and 27 mm TSE on the basis of scaling.

Figure 4.13 shows the effect of processing with identical DF in the two extruders on the TSWG process. For both extruders, it was noticed that the granule size (d_{90}) was reduced with the rise of DF at the same amount. The span of PSD was increased for the small-size extruder and decreased for the large-size extruder when the DF at the same level was increased. For smaller extruder, the granule fracture strength was increased for rising the DF inside the extruder barrel. Overall, the consistency in the granule size (d_{90}), span, and fracture strength were increased when the DF was increased at the same level inside the barrel of the two extruders. From the above analysis, it can be pointed out that the effect of Péclet number and Reynolds number for scale-up of TSWG on the twin-screw extruder was helpful, but it could not make perfect understanding of scaling. On the other hand, the scaling worked well and brought more sense when the DF was fixed in the 18 mm and 27 mm twin-screw extruders.

CHAPTER 5: CONCLUSION

The TSWG process allows continuous processing to produce consistent quality products and efficient scaling-up maintains that consistency within a process window and between different-sized machines. The present study analyzed the scaling possibility of granulation properties between two common sizes of twin-screw extruders in pharmaceutical manufacturing for a control formulation under certain conditions. This study was completed based on the process mechanisms involving compaction and mixing to develop a set of scaling rules, and the experimental findings of 18 mm and 27 mm twin-screw extruders. Two dimensionless parameters such as the Reynolds number and Péclet number were identified and examined for scaling of two geometrically similar extruders using a sustained release formulation. The kinetical and dynamical similarities of the two extruders were controlled by adjusting process parameters such as powder feed rate and screw speed based on the Reynolds number and Péclet number.

Significant work was undertaken to understand the impact of powder feed rate, screw speed, liquid-to-solid ratio, and extruder size on the mean residence time of the particles, degree of barrel fill, granule size, particle size distribution, and granule strength. When other dimensionless parameters were taken constant, the extruder size had a meaningful effect on the granule properties with an almost linear relationship found between the extruder diameter and the granule size (d_{90}). The dimensionless Reynolds number (and screw speed) seemed to have the least influence on the wet granulation process while the Péclet number (and powder feed rate) had the great influence on the granule properties for both small- and large-size extruders though it was mostly dependent on the degree of fill. The degree of fill calculated from the mean residence time of the particles appeared to cause the most significant changes in the

granule properties. Powder feed rate, extruder size, and liquid-to-solid ratio had meaningful influences on the degree of fill, mixing intensity, and compaction inside the extruder barrel, which controlled the d_{90}, span of PSD, and fracture strength of granules.

A core part of this thesis focused on establishing scaling rules based on Genetic programming, which developed symbolic regression models to explore important relationships between the two dimensionless groups and the granule properties. These fitting models revealed both linear and nonlinear behaviors in the relationships based on extruder diameter. A scaling law for d_{90} was chosen to represent PSD because the other moments showed little variations for varying process parameters. The sensitivity analysis identified a realistic evaluation range for the two dimensionless numbers which were varied between their extremes to observe different sensitivities in the d_{90}, span, and fracture strength of granules for the two extruders. The extruder size greatly influenced the fits for the granule properties in the two machines, which was desired to have robust scaling rules, although the fits showed only moderate accuracy due to the limited amount of data available for GP modeling. Because of its significant contribution to the process, the degree of fill was identified as a vital aspect of granulation in this study which was assumed as constant between two extruders to analyze the impact of scaling laws as well as to examine how the scaling worked to retain consistency in the granule properties. The consistency in the granule properties was improved when the degree of fill at the same amount in the two machines was increased. The scaling rules developed from the Genetic programming to scale up the TSWG system from small-scale to large-scale allow for identifying the new powder feed rate and screw speed in advance to maintain uniformity in the processes and produce granules of desired quality.

The present work is essential to understanding the twin-screw wet granulation process, as the findings of the work have provided insight into the mechanism of the process as well as the mixing performance, which is a great use for further research to improve the understanding of the granulation process in the twin-screw extruder. The following recommendations are made for future work:

- Comparing the scalability of the TSWG process on the twin-screw extruder using different formulations, correlating mixing intensity with granule properties, and establishing the scaling-up rules.

- Comparing mixing performances of wet granulation on the twin-screw extruder with a varying screw configuration containing different angle kneading blocks and monitoring torque, process temperature, pressure, and exit temperature during granulation by combining PAT tools with the continuous process.

- Correlating mixing performance with drug product quality attributes, such as compressibility, the strength of resultant tablets, and their dissolution rate, using appropriate formulations to fulfill the wide-ranging goal of QbD.

- Introducing other AI tools such as Artificial neural networks and comparing them with GP for modeling the TSWG system to predict granule properties on different scales of the twin-screw extruder.

References

[1] J. G. Osorio *et al.*, "Scaling of continuous twin screw wet granulation," *AIChE J.*, vol. 63, no. 3, pp. 921–932, 2017, doi: 10.1002/aic.15459.

[2] S. Shanmugam, "Granulation techniques and technologies: Recent progresses," *BioImpacts*, vol. 5, no. 1, pp. 55–63, 2015, doi: 10.15171/bi.2015.04.

[3] S. P. Forster, E. Dippold, and T. Chiang, "Twin-Screw Melt Granulation for Oral Solid Pharmaceutical Products," 2021.

[4] C. M. McTaggart, J. A. Ganley, A. Sickmueller, and S. E. Walker, "The evaluation of formulation and processing conditions of a melt granulation process," *Int. J. Pharm.*, vol. 19, no. 2, pp. 139–148, 1984, doi: 10.1016/0378-5173(84)90156-X.

[5] T. Liu, N. Kittikunakorn, Y. Zhang, and F. Zhang, "Mechanisms of twin screw melt granulation," *J. Drug Deliv. Sci. Technol.*, vol. 61, no. August 2020, p. 102150, 2021, doi: 10.1016/j.jddst.2020.102150.

[6] A. Kumar *et al.*, "Mixing and transport during pharmaceutical twin-screw wet granulation: Experimental analysis via chemical imaging," *Eur. J. Pharm. Biopharm.*, vol. 87, no. 2, pp. 279–289, 2014, doi: 10.1016/j.ejpb.2014.04.004.

[7] M. R. Thompson and J. Sun, "Wet granulation in a twin-screw extruder: Implications of screw design," *J. Pharm. Sci.*, vol. 99, no. 4, pp. 2090–2103, 2010, doi: 10.1002/jps.21973.

[8] R. M. Dhenge, J. J. Cartwright, D. G. Doughty, M. J. Hounslow, and A. D. Salman, "Twin screw wet granulation: Effect of powder feed rate," *Adv. Powder Technol.*, vol. 22, no. 2, pp. 162–166, Mar. 2011, doi: 10.1016/j.apt.2010.09.004.

[9] T. C. Seem *et al.*, "Twin screw granulation — A literature review," *Powder Technol.*, vol. 276, pp. 89–102, May 2015, doi: 10.1016/J.POWTEC.2015.01.075.

[10] M. R. Thompson and K. P. O'Donnell, "'Rolling' phenomenon in twin screw granulation with controlled-release excipients," *Drug Dev. Ind. Pharm.*, vol. 41, no. 3, pp. 482–492, 2015, doi: 10.3109/03639045.2013.879723.

[11] O. R. Arndt and P. Kleinebudde, "Influence of binder properties on dry granules and tablets," *Powder Technol.*, vol. 337, pp. 68–77, Sep. 2018, doi: 10.1016/j.powtec.2017.04.054.

[12] C. K. Sahoo, S. R. M. Rao, M. Sudhakar, and J. Bhaskar, "Advances in granulation technology," *Res. J. Pharm. Technol.*, vol. 9, no. 5, pp. 571–580, 2016, doi: 10.5958/0974-360X.2016.00108.6.

[13] T. Plath, C. Korte, R. Sivanesapillai, and T. Weinhart, "Parametric study of residence time distributions and granulation kinetics as a basis for process modeling of twin-screwwet granulation," *Pharmaceutics*, vol. 13, no. 5, 2021, doi: 10.3390/pharmaceutics13050645.

[14] T. Osamura *et al.*, "Formulation design of granules prepared by wet granulation method using a multi-functional single-punch tablet press to avoid tableting failures," *Asian J. Pharm. Sci.*, vol. 13, no. 2, pp. 113–119, 2018, doi: 10.1016/j.ajps.2017.08.002.

[15] N. Kittikunakorn, T. Liu, and F. Zhang, "Twin-screw melt granulation: Current

progress and challenges," *Int. J. Pharm.*, vol. 588, no. May, p. 119670, 2020, doi: 10.1016/j.ijpharm.2020.119670.

[16] D. Djuric, B. Van Melkebeke, P. Kleinebudde, J. P. Remon, and C. Vervaet, "Comparison of two twin-screw extruders for continuous granulation," *Eur. J. Pharm. Biopharm.*, vol. 71, no. 1, pp. 155–160, Jan. 2009, doi: 10.1016/j.ejpb.2008.06.033.

[17] M. R. Thompson, "Twin screw granulation-review of current progress," *Drug Dev. Ind. Pharm.*, vol. 41, no. 8, pp. 1223–1231, 2015, doi: 10.3109/03639045.2014.983931.

[18] T. Liu, N. Kittikunakorn, Y. Zhang, and F. Zhang, "Mechanisms of twin screw melt granulation," *J. Drug Deliv. Sci. Technol.*, vol. 61, no. October 2020, p. 102150, doi: 10.1016/j.jddst.2020.102150.

[19] X. Ye *et al.*, "Effects of Processing on a Sustained Release Formulation Prepared by Twin-Screw Dry Granulation," *J. Pharm. Sci.*, vol. 108, no. 9, pp. 2895–2904, 2019, doi: 10.1016/j.xphs.2019.04.004.

[20] K. E. Steffens, M. B. Brenner, M. U. Hartig, M. Monschke, and K. G. Wagner, "Melt granulation: A comparison of granules produced via high-shear mixing and twin-screw granulation," *Int. J. Pharm.*, vol. 591, no. October, p. 119941, 2020, doi: 10.1016/j.ijpharm.2020.119941.

[21] N. Kittikunakorn, L. Extrusion, and F. Zhang, "PROCESSES, CHALLENGES, AND THE FUTURE OF TWIN-SCREW GRANULATION FOR MANUFACTURING ORAL TABLETS AND CAPSULES Adopting twin screw granulation can aid in the transition from batch to continuous processes for pharmaceuticals."

[22] N. Kittikunakorn, C. C. Sun, and F. Zhang, "Effect of screw profile and processing conditions on physical transformation and chemical degradation of gabapentin during twin-screw melt granulation," *Eur. J. Pharm. Sci.*, vol. 131, no. January, pp. 243–253, 2019, doi: 10.1016/j.ejps.2019.02.024.

[23] R. M. Dhenge, R. S. Fyles, J. J. Cartwright, D. G. Doughty, M. J. Hounslow, and A. D. Salman, "Twin screw wet granulation: Granule properties," *Chem. Eng. J.*, vol. 164, no. 2–3, pp. 322–329, 2010, doi: 10.1016/j.cej.2010.05.023.

[24] M. Fonteyne *et al.*, "Real-time assessment of critical quality attributes of a continuous granulation process," *Pharm. Dev. Technol.*, vol. 18, no. 1, pp. 85–97, 2013, doi: 10.3109/10837450.2011.627869.

[25] N. Willecke, A. Szepes, M. Wunderlich, J. P. Remon, C. Vervaet, and T. De Beer, "A novel approach to support formulation design on twin screw wet granulation technology: Understanding the impact of overarching excipient properties on drug product quality attributes," *Int. J. Pharm.*, vol. 545, no. 1–2, pp. 128–143, 2018, doi: 10.1016/j.ijpharm.2018.04.017.

[26] R. M. Dhenge, J. J. Cartwright, M. J. Hounslow, and A. D. Salman, "Twin screw wet granulation: Effects of properties of granulation liquid," *Powder Technol.*, vol. 229, pp. 126–136, Oct. 2012, doi: 10.1016/J.POWTEC.2012.06.019.

[27] T. C. Seem *et al.*, "Twin screw granulation - A literature review," *Powder Technology*, vol. 276. Elsevier, pp. 89–102, May 01, 2015, doi: 10.1016/j.powtec.2015.01.075.

[28] M. Maniruzzaman, S. A. Ross, T. Dey, A. Nair, M. J. Snowden, and D. Douroumis, "A quality by design (QbD) twin—Screw extrusion wet granulation approach for processing water insoluble drugs," *Int. J. Pharm.*, vol. 526, no. 1–2, pp. 496–505,

2017, doi: 10.1016/j.ijpharm.2017.05.020.

[29] L. Tan, A. J. Carella, Y. Ren, and J. B. Lo, "Process optimization for continuous extrusion wet granulation," *Pharm. Dev. Technol.*, vol. 16, no. 4, pp. 302–315, Aug. 2011, doi: 10.3109/10837451003692587.

[30] C. Zheng, L. Zhang, N. Govender, and C. Y. Wu, "DEM analysis of residence time distribution during twin screw granulation," *Powder Technol.*, vol. 377, pp. 924–938, 2021, doi: 10.1016/j.powtec.2020.09.049.

[31] B. Johansson and G. Alderborn, "The effect of shape and porosity on the compression behaviour and tablet forming ability of granular materials formed from microcrystalline cellulose," *Eur. J. Pharm. Biopharm.*, vol. 52, no. 3, pp. 347–357, 2001, doi: 10.1016/S0939-6411(01)00186-2.

[32] B. Van Melkebeke, C. Vervaet, and J. P. Remon, "Validation of a continuous granulation process using a twin-screw extruder," *Int. J. Pharm.*, vol. 356, no. 1–2, pp. 224–230, May 2008, doi: 10.1016/j.ijpharm.2008.01.012.

[33] H. Li, M. R. Thompson, and K. P. O'Donnell, "Understanding wet granulation in the kneading block of twin screw extruders," *Chem. Eng. Sci.*, vol. 113, pp. 11–21, 2014, doi: 10.1016/j.ces.2014.03.007.

[34] A. Batra, D. Desai, and A. T. M. Serajuddin, "Investigating the Use of Polymeric Binders in Twin Screw Melt Granulation Process for Improving Compactibility of Drugs," *J. Pharm. Sci.*, vol. 106, no. 1, pp. 140–150, 2017, doi: 10.1016/j.xphs.2016.07.014.

[35] W. Meng *et al.*, "Statistical analysis and comparison of a continuous high shear granulator with a twin screw granulator: Effect of process parameters on critical granule attributes and granulation mechanisms," *Int. J. Pharm.*, vol. 513, no. 1–2, pp. 357–375, 2016, doi: 10.1016/j.ijpharm.2016.09.041.

[36] B. Mu and M. R. Thompson, "Examining the mechanics of granulation with a hot melt binder in a twin-screw extruder," *Chem. Eng. Sci.*, vol. 81, pp. 46–56, 2012, doi: 10.1016/j.ces.2012.06.057.

[37] J. Wesholowski, K. Hoppe, K. Nickel, C. Muehlenfeld, and M. Thommes, "Scale-Up of pharmaceutical Hot-Melt-Extrusion: Process optimization and transfer," *Eur. J. Pharm. Biopharm.*, vol. 142, no. July, pp. 396–404, 2019, doi: 10.1016/j.ejpb.2019.07.009.

[38] A. M. Agrawal and P. Pandey, "Scale Up of Pan Coating Process Using Quality by Design Principles," *J. Pharm. Sci.*, vol. 104, no. 11, pp. 3589–3611, 2015, doi: 10.1002/jps.24582.

[39] A. S. Narang, T. Stevens, K. Macias, S. Paruchuri, Z. Gao, and S. Badawy, "Application of In-line Focused Beam Reflectance Measurement to Brivanib Alaninate Wet Granulation Process to Enable Scale-up and Attribute-based Monitoring and Control Strategies," *J. Pharm. Sci.*, vol. 106, no. 1, pp. 224–233, 2017, doi: 10.1016/j.xphs.2016.08.025.

[40] P. Suresh, I. Sreedhar, R. Vaidhiswaran, and A. Venugopal, "A comprehensive review on process and engineering aspects of pharmaceutical wet granulation," *Chem. Eng. J.*, vol. 328, pp. 785–815, 2017, doi: 10.1016/j.cej.2017.07.091.

[41] M. Richter and T. Fisher, "Continuous twin-screw granulation – What to consider in process design, development and scale-up."

[42] S. Pohl and P. Kleinebudde, "A review of regime maps for granulation," *Int. J. Pharm.*, vol. 587, no. March, p. 119660, 2020, doi: 10.1016/j.ijpharm.2020.119660.

[43] P. Barmpalexis, K. Kachrimanis, A. Tsakonas, and E. Georgarakis, "Symbolic regression via genetic programming in the optimization of a controlled release pharmaceutical formulation," *Chemom. Intell. Lab. Syst.*, vol. 107, no. 1, pp. 75–82, 2011, doi: 10.1016/j.chemolab.2011.01.012.

[44] D. Q. Do, R. C. Rowe, and P. York, "Modelling drug dissolution from controlled release products using genetic programming," *Int. J. Pharm.*, vol. 351, no. 1–2, pp. 194–200, 2008, doi: 10.1016/j.ijpharm.2007.09.044.

[45] A. Fouladitajar, F. Zokaee Ashtiani, A. Okhovat, and B. Dabir, "Membrane fouling in microfiltration of oil-in-water emulsions; a comparison between constant pressure blocking laws and genetic programming (GP) model," *Desalination*, vol. 329, pp. 41–49, 2013, doi: 10.1016/j.desal.2013.09.003.

[46] P. Kazemi *et al.*, "Computational intelligence modeling of granule size distribution for oscillating milling," *Powder Technol.*, vol. 301, pp. 1252–1258, 2016, doi: 10.1016/j.powtec.2016.07.046.

[47] A. F. Silva *et al.*, "Process monitoring and evaluation of a continuous pharmaceutical twin-screw granulation and drying process using multivariate data analysis," *Eur. J. Pharm. Biopharm.*, vol. 128, no. April, pp. 36–47, 2018, doi: 10.1016/j.ejpb.2018.04.011.

[48] H. Lou, B. Lian, and M. J. Hageman, "Applications of Machine Learning in Solid Oral Dosage Form Development," *J. Pharm. Sci.*, vol. 110, no. 9, pp. 3150–3165, 2021, doi: 10.1016/j.xphs.2021.04.013.

[49] C. Portier *et al.*, "Continuous twin screw granulation: Impact of microcrystalline cellulose batch-to-batch variability during granulation and drying – A QbD approach," *Int. J. Pharm. X*, vol. 3, Dec. 2021, doi: 10.1016/j.ijpx.2021.100077.

[50] A. T. O. Andrade, "Application of multivariate techniques in the evaluation of melt granulation products," *Brazilian J. Pharm. Sci.*, vol. 47, no. 4, pp. 733–741, 2011, doi: 10.1590/S1984-82502011000400010.

[51] T. Liu *et al.*, "Physicochemical changes and chemical degradation of gliclazide during twin-screw melt granulation," *Int. J. Pharm.*, vol. 619, no. February, p. 121702, 2022, doi: 10.1016/j.ijpharm.2022.121702.

[52] A. Tsakonas, "A comparison of classification accuracy of four genetic programming-evolved intelligent structures," *Inf. Sci. (Ny).*, vol. 176, no. 6, pp. 691–724, 2006, doi: 10.1016/j.ins.2005.03.012.

[53] A. Tsakonas and G. Dounias, "Evolving neural-symbolic systems guided by adaptive training schemes: Applications in finance," *Appl. Artif. Intell.*, vol. 21, no. 7, pp. 681–706, 2007, doi: 10.1080/08839510701492603.

[54] A. Chavoya, C. Lopez-Martin, I. R. Andalon-Garcia, and M. E. Meda-Campaña, "Genetic Programming as Alternative for Predicting Development Effort of Individual Software Projects," *PLoS One*, vol. 7, no. 11, 2012, doi: 10.1371/journal.pone.0050531.

[55] P. Barmpalexis, K. Kachrimanis, and E. Georgarakis, "Solid dispersions in the development of a nimodipine floating tablet formulation and optimization by artificial neural networks and genetic programming," *Eur. J. Pharm. Biopharm.*, vol. 77, no. 1,

pp. 122–131, 2011, doi: 10.1016/j.ejpb.2010.09.017.

[56]   P. Barmpalexis, A. Karagianni, G. Karasavvaides, and K. Kachrimanis, "Comparison of multi-linear regression, particle swarm optimization artificial neural networks and genetic programming in the development of mini-tablets," *Int. J. Pharm.*, vol. 551, no. 1–2, pp. 166–176, 2018, doi: 10.1016/j.ijpharm.2018.09.026.

[57]   M. Landin, "Artificial Intelligence Tools for Scaling Up of High Shear Wet Granulation Process," *J. Pharm. Sci.*, vol. 106, no. 1, pp. 273–277, 2017, doi: 10.1016/j.xphs.2016.09.022.

[58]   T. M. Lee *et al.*, "Prediction of membrane fouling in the pilot-scale microfiltration system using genetic programming," *Desalination*, vol. 247, no. 1–3, pp. 285–294, 2009, doi: 10.1016/j.desal.2008.12.031.

[59]   S. Ji, "A generalized mixture rule for estimating the viscosity of solid-liquid suspensions and mechanical properties of polyphase rocks and composite materials," *J. Geophys. Res. Solid Earth*, vol. 109, no. 10, pp. 1–18, 2004, doi: 10.1029/2004JB003124.

[60]   S. Ji, Q. Wang, B. Xia, and D. Marcotte, "Mechanical properties of multiphase materials and rocks: A phenomenological approach using generalized means," *J. Struct. Geol.*, vol. 26, no. 8, pp. 1377–1390, 2004, doi: 10.1016/j.jsg.2003.12.004.

[61]   Z. Yang, S. Xiaoxia, and M. Wenjun, "Research on the axial velocity of the raw coal particles in vertical screw conveyor by using the discrete element method," *J. Mech. Sci. Technol.*, vol. 35, no. 6, pp. 2551–2560, 2021, doi: 10.1007/s12206-021-0526-z.

[62]   A. H. Sabri, C. N. Hallam, N. A. Baker, D. S. Murphy, and I. P. Gabbott, "Understanding tablet defects in commercial manufacture and transfer," *J. Drug Deliv. Sci. Technol.*, vol. 46, no. May, pp. 1–6, 2018, doi: 10.1016/j.jddst.2018.04.020.

[63]   M. J. Adams, M. A. Mullier, and J. P. K. Seville, "Agglomerate strength measurement using a uniaxial confined compression test," *Powder Technol.*, vol. 78, no. 1, pp. 5–13, 1994, doi: 10.1016/0032-5910(93)02777-8.

[64]   F. Nicklasson and G. Alderborn, "Analysis of the compression mechanics of pharmaceutical agglomerates of different porosity and composition using the Adams and Kawakita equations," *Pharm. Res.*, vol. 17, no. 8, pp. 949–954, 2000, doi: 10.1023/A:1007575120817.

[65]   J. Fu, G. K. Reynolds, M. J. Adams, M. J. Hounslow, and A. D. Salman, "An experimental study of the impact breakage of wet granules," *Chem. Eng. Sci.*, vol. 60, no. 14, pp. 4005–4018, 2005, doi: 10.1016/j.ces.2005.02.037.

Appendix

A.1 Influence of Re and Pe on Residence Time Distribution (RTD)
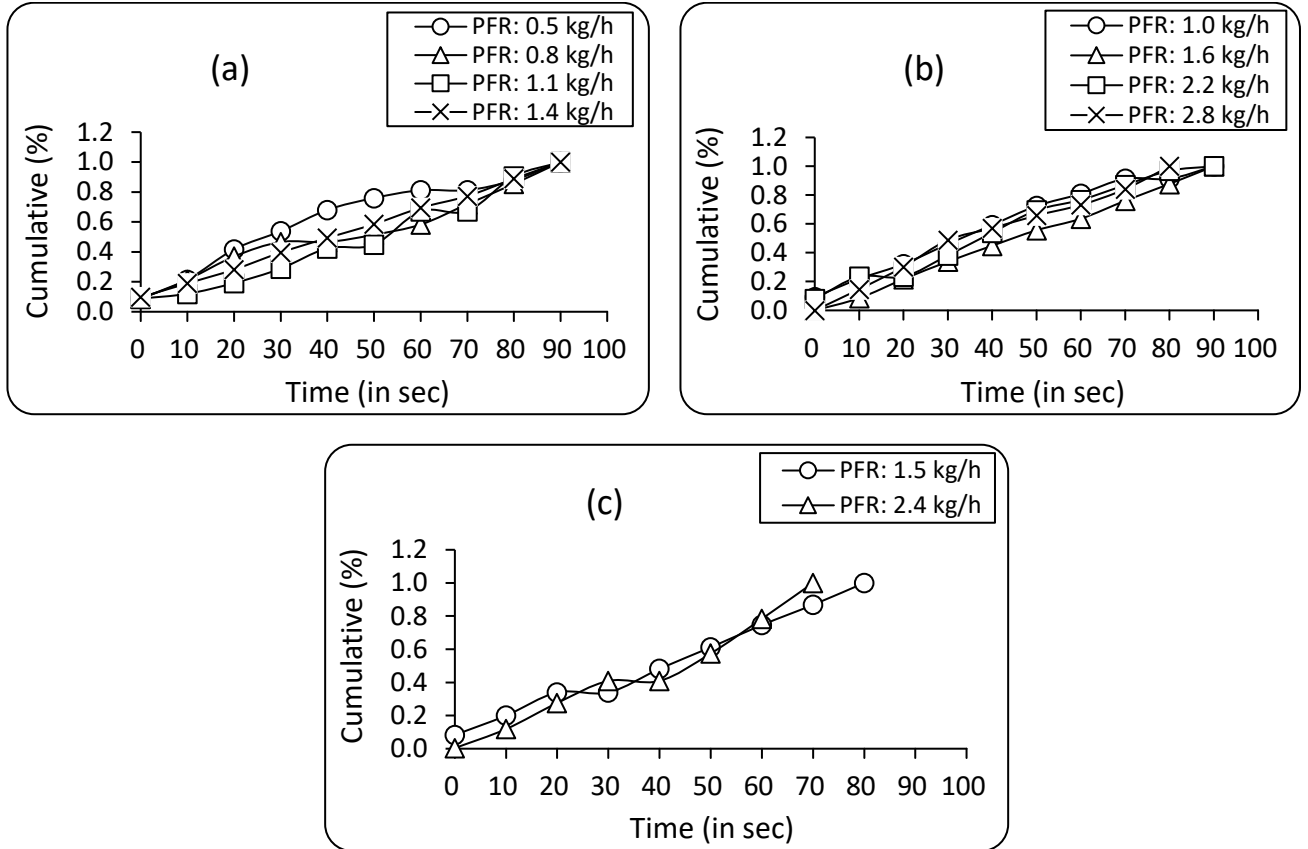

Figure A.1. Effect of Powders feed rate (PFR) on RTD with D = 18 mm at (a) 100 rpm, (b) 200 rpm, and (c) 300 rpm (for 26% L/S ratio)
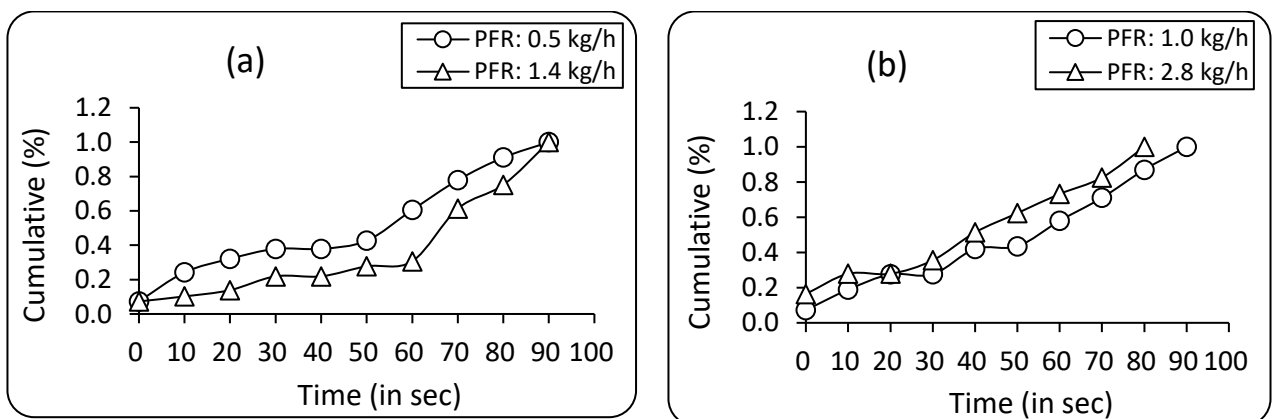

Figure A.2. Effect of Powders feed rate (PFR) on RTD with D = 18 mm at (a) 100 rpm and (b) 200 rpm (for 30% L/S ratio)
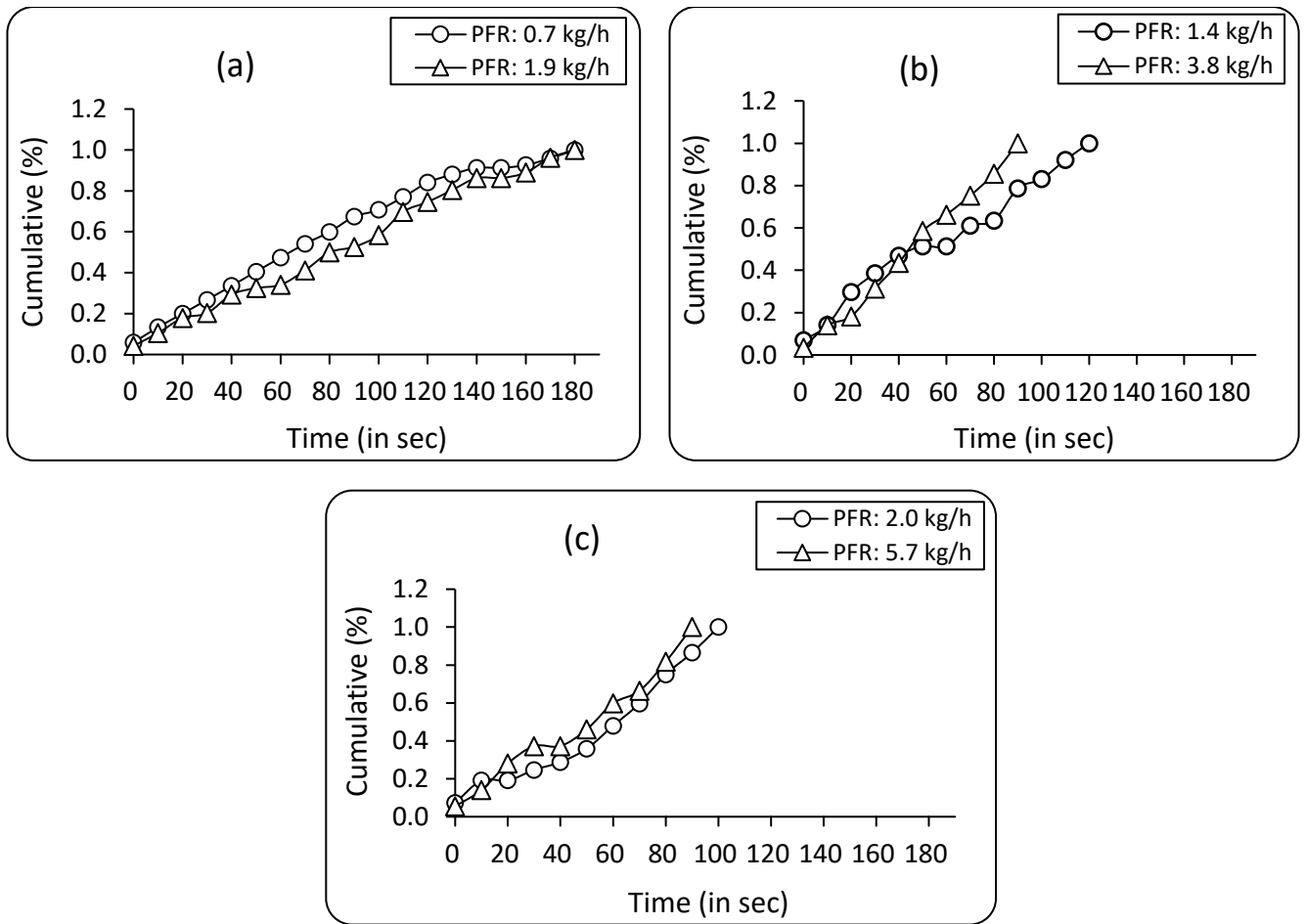
Figure A.3. Effect of Powders feed rate (PFR) on RTD with D = 27 mm at (a) 39 rpm, (b) 78 rpm, and (c) 117 rpm (for 26% L/S ratio)
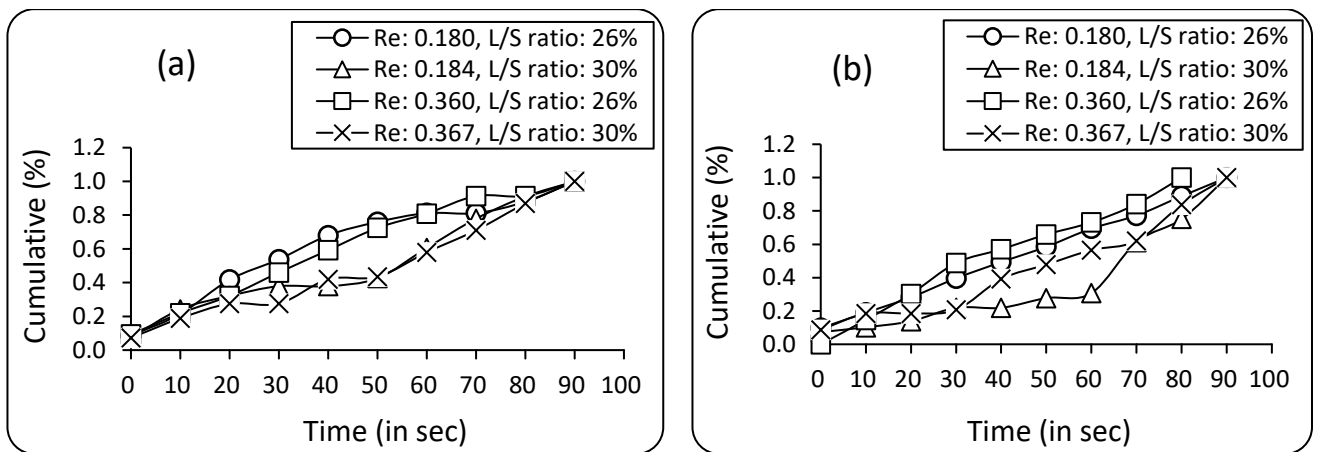

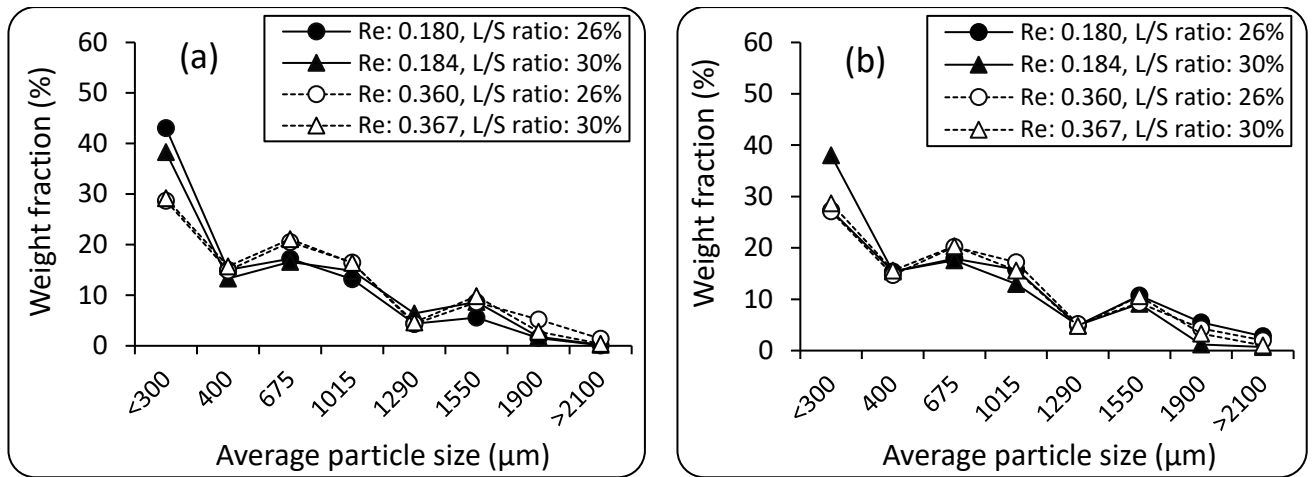*Figure A.4. Effect of Reynolds number (Re) with varying L/S ratio (%) on RTD with D = 18 mm at (a) Pe = 13.242 and (b) Pe = 4.729*
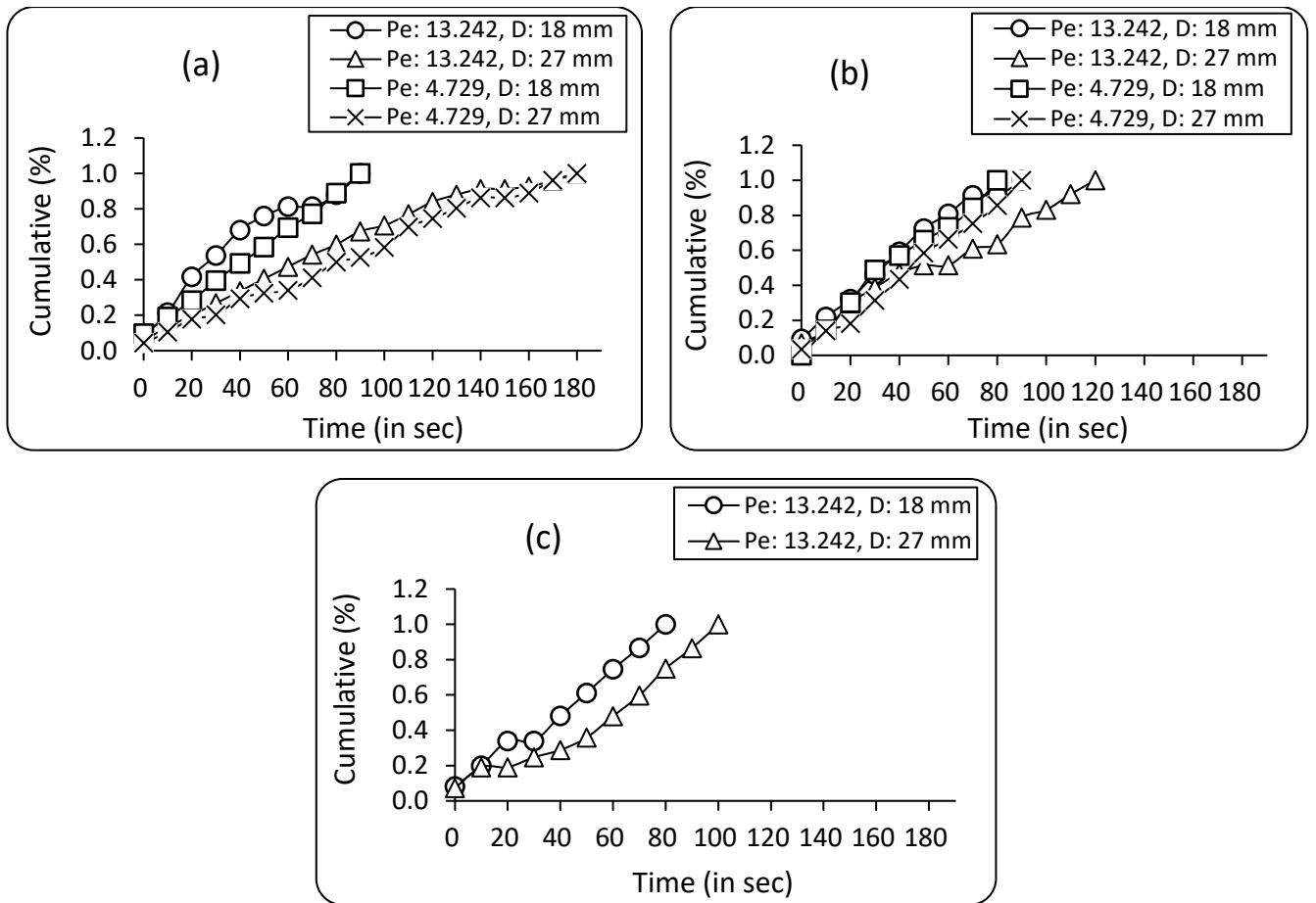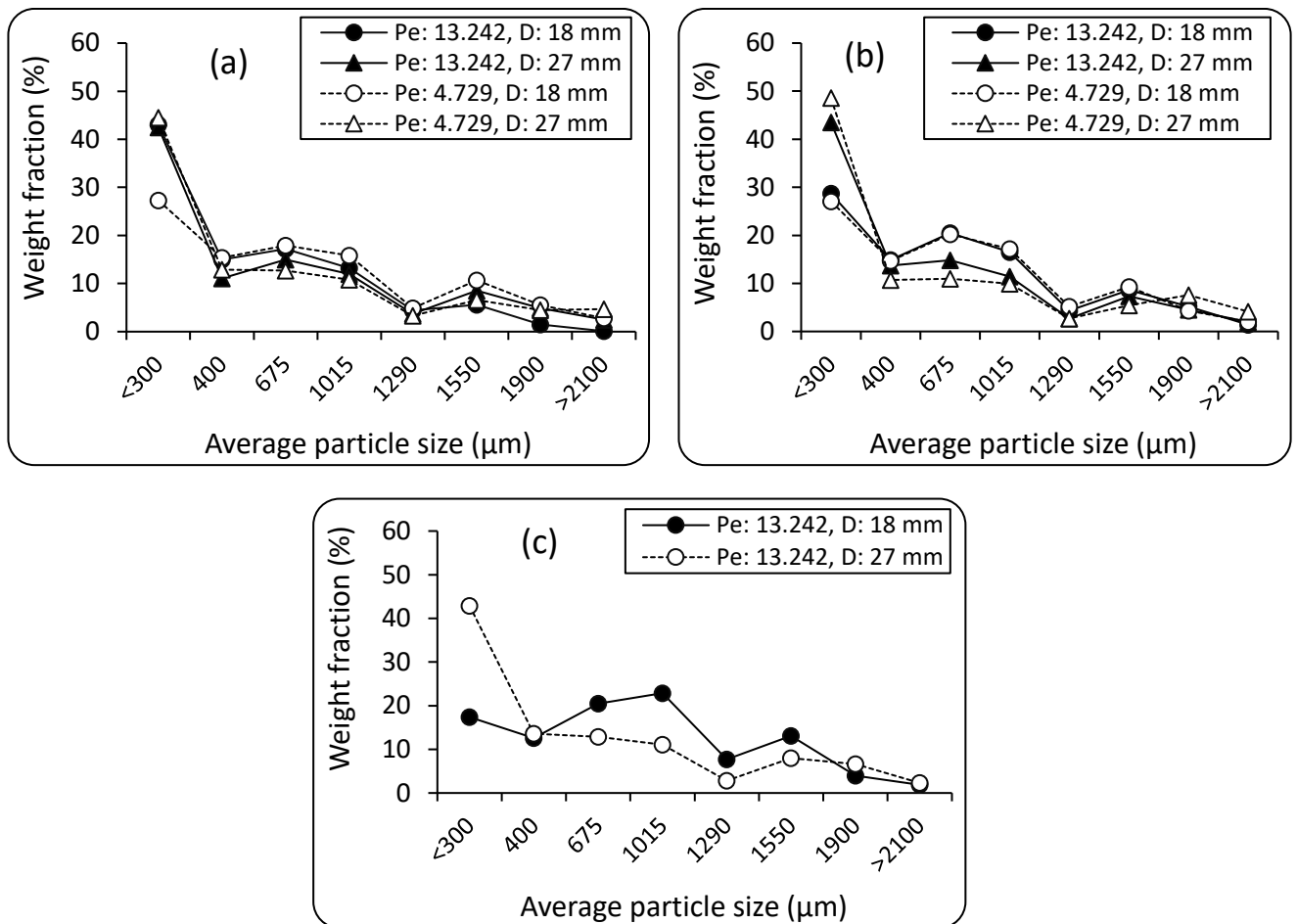
Figure A.5. Effects of Extruder barrel diameter (D) and Péclet number (Pe) on RTD with 26% L/S ratio at (a) Re = 0.180, (b) Re = 0.360, and (c) Re = 0.541

A.2 Influence of Re and Pe on Mean Residence Time (MRT)
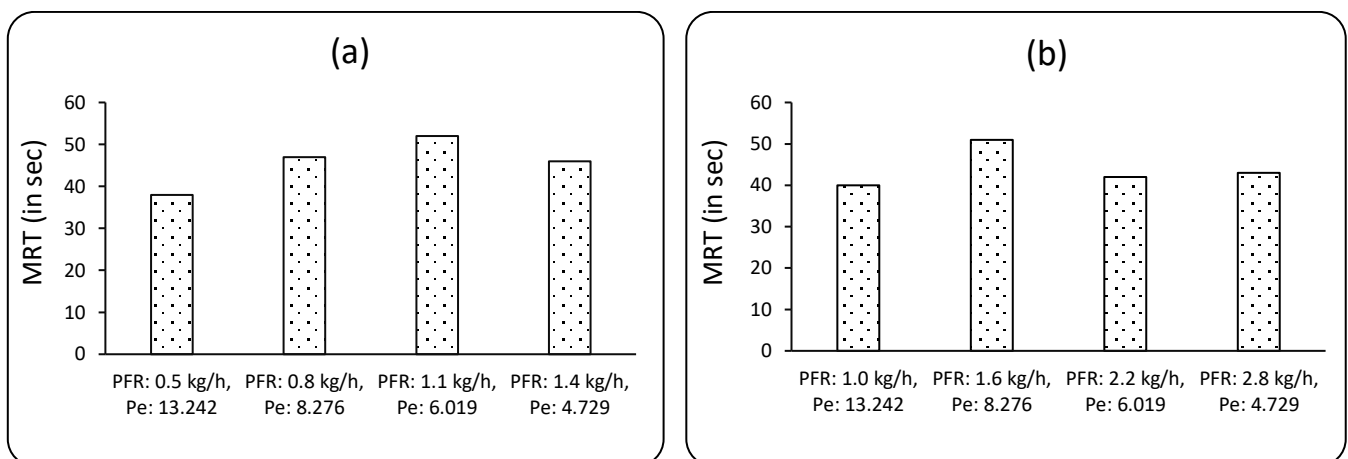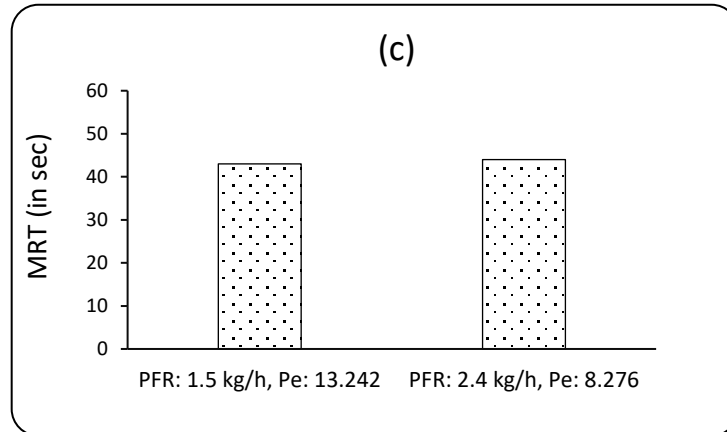
Figure A.6. Effect of Powder feed rate (PFR) and associated Péclet number (Pe) on MRT with D = 18 mm at (a) Re = 0.180, (b) Re = 0.360, and (c) Re = 0.541 (for 26% L/S ratio) [for D = 18 mm with 26% L/S ratio, RSE for MRT = 1.416]

A.3 Influence of Re and Pe on Particle Size Distribution (PSD)
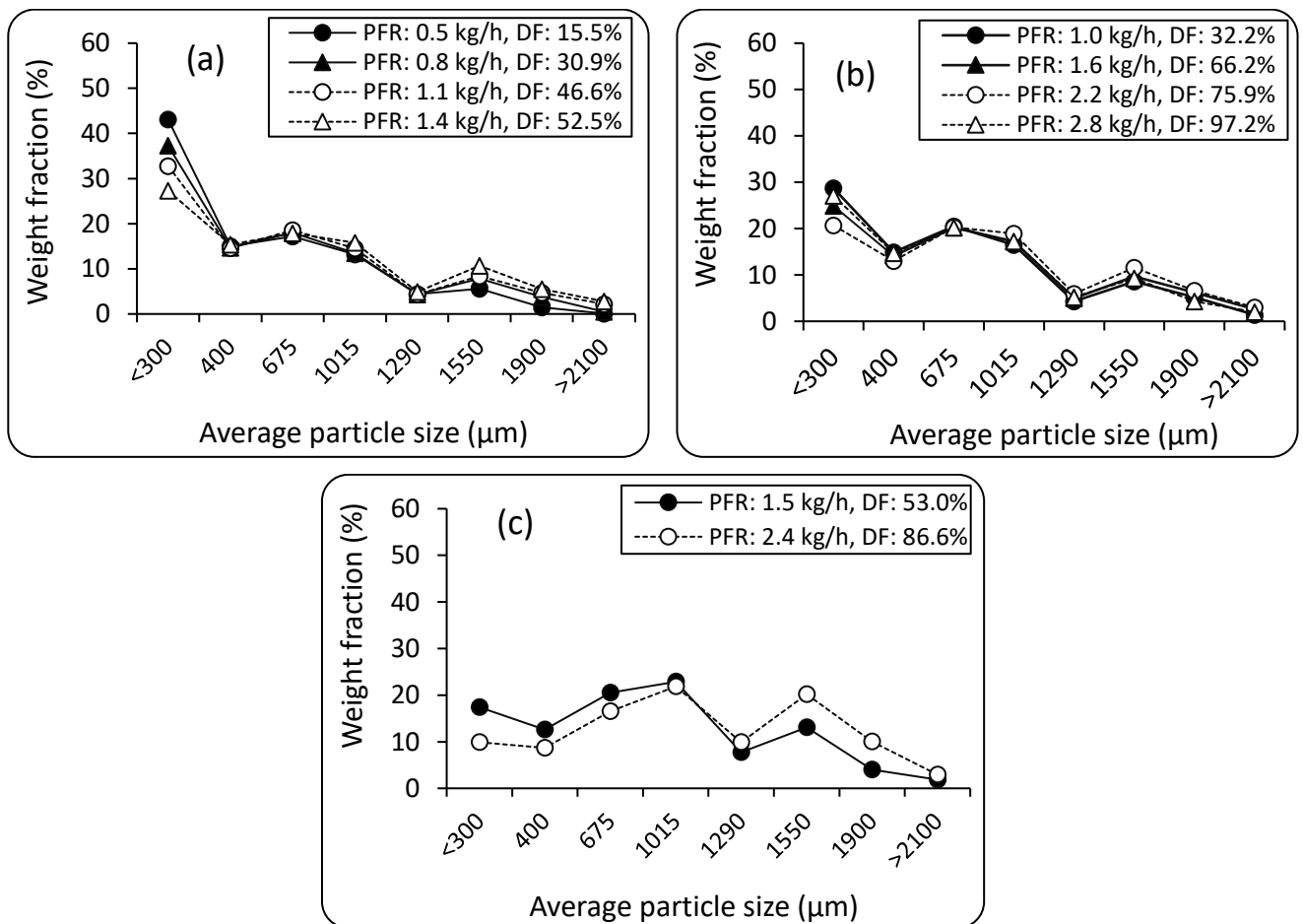
Figure A.7. Effect of Degree of fill (DF) with varying Powder feed rate (PFR) on PSD with D = 18 mm at (a) Re = 0.180, (b) Re = 0.360, and (c) Re = 0.541 (for 26% L/S ratio)
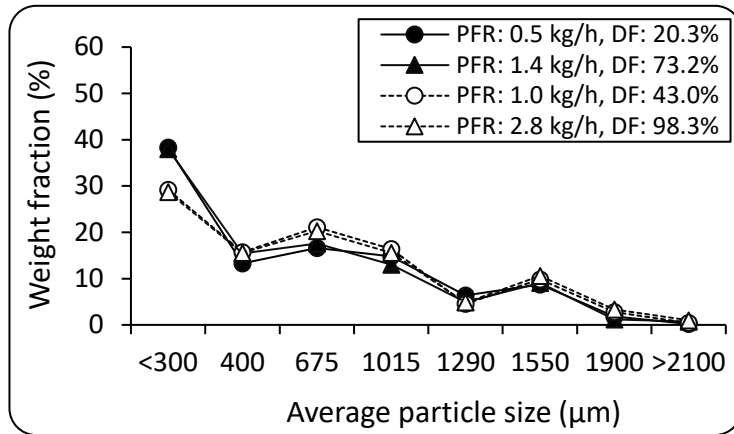
Figure A.8. Effect of Degree of fill (DF) with varying Powder feed rate (PFR) on PSD with D = 18 mm at Re = 0.184 and Re = 0.367 (for 30% L/S ratio)
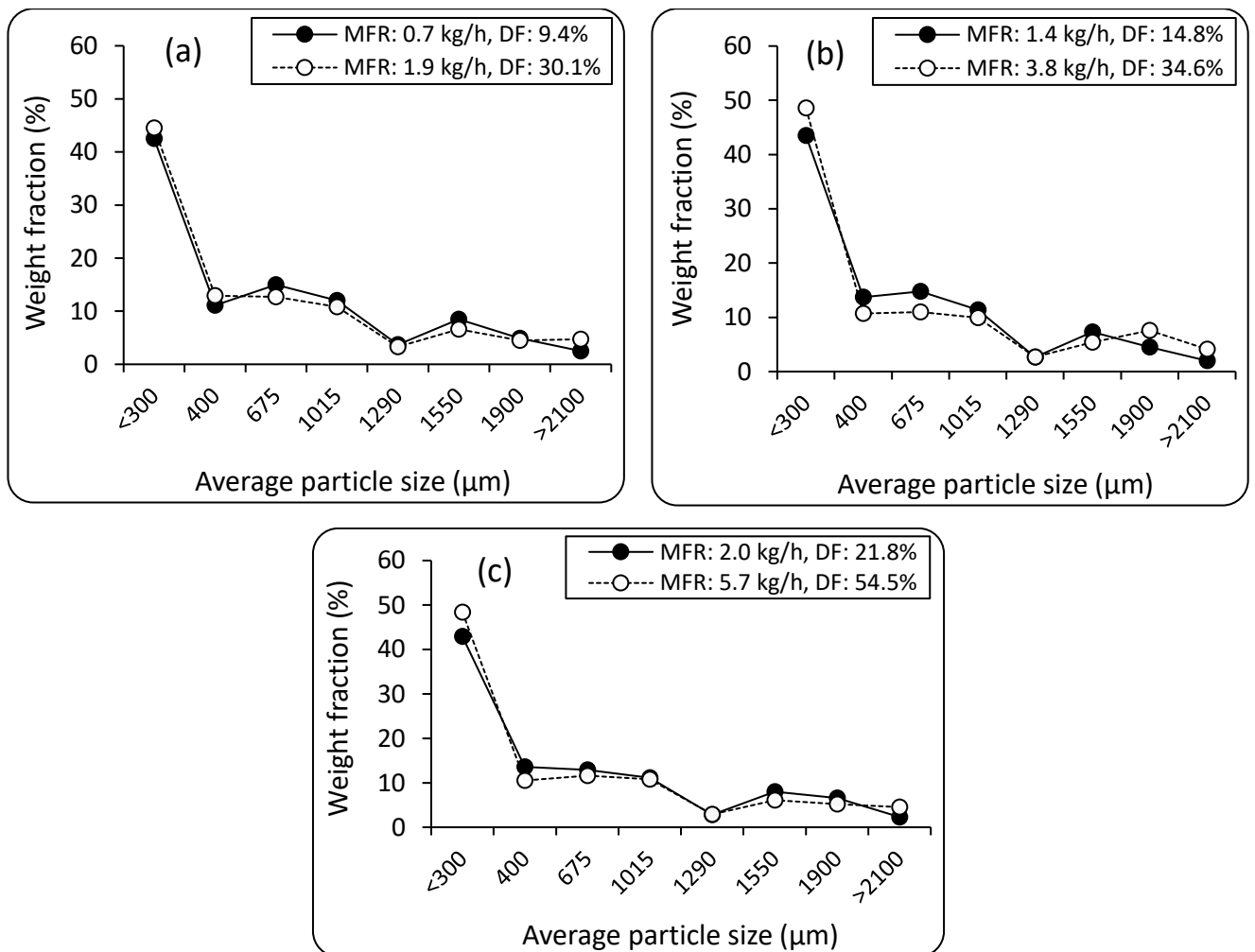
Figure A.9. Effect of Degree of fill (DF) with varying Powder feed rate (PFR) on PSD with D = 27 mm at (a) Re = 0.180, (b) Re = 0.360, and (c) Re = 0.541 (for 26% L/S ratio)

Figure A.10. Effect of Reynolds number (Re) with varying L/S ratio (%) on PSD with D = 18 mm at (a) Pe = 13.242 and (b) Pe = 4.729

Figure A.11. Effect of Extruder barrel diameter (D) and Péclet number (Pe) on PSD with 26% L/S ratio at (a) Re = 0.180, (b) Re = 0.360, and (c) Re = 0.541

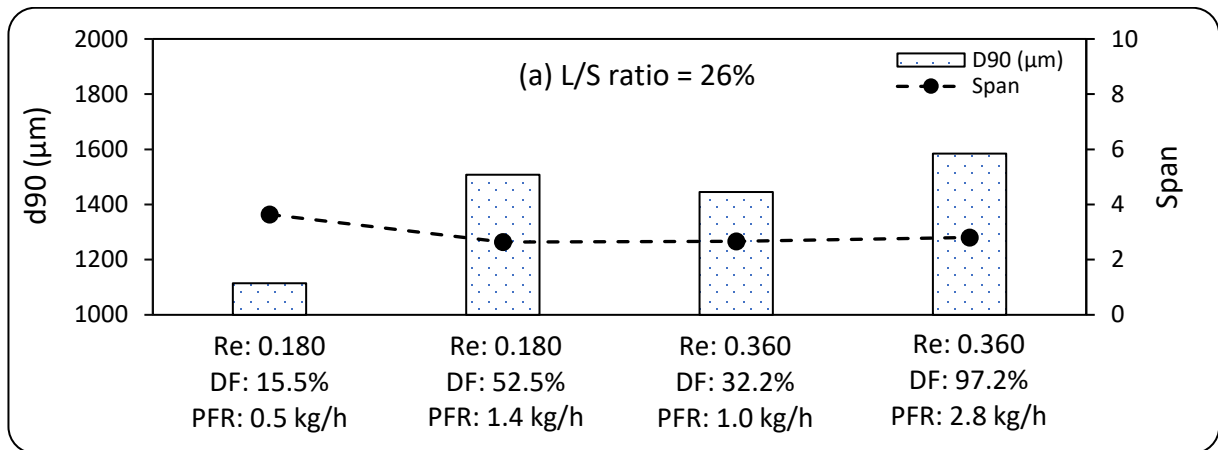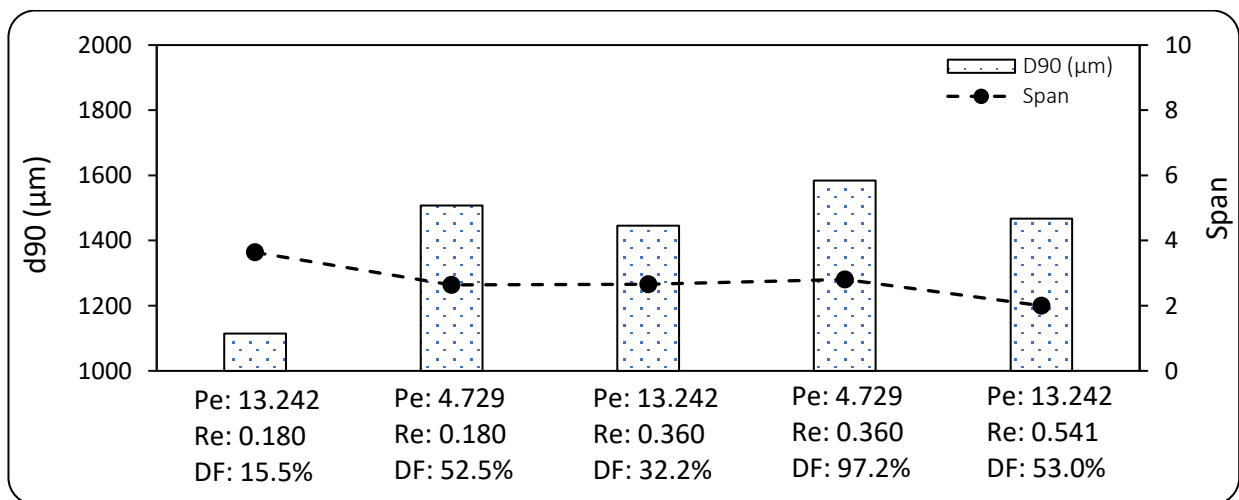## A.4 Influence of Re and Pe on d_{90} and Span of PSD
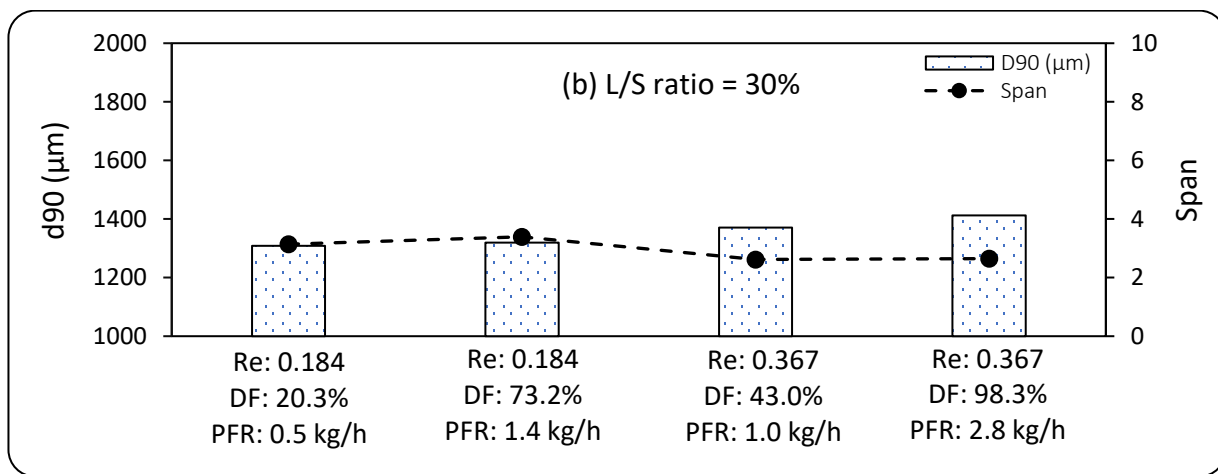
Figure A.12. Effect of Degree of fill (DF) and Reynolds number (Re) on d_{90} and Span with D = 18 mm at (a) 26% L/S ratio and (b) 30% L/S ratio [for 26% L/S ratio, RSE for d_{90} & Span =46.442 & 0.188 and for 30% L/S ratio, RSE for d_{90} & Span =24.001 & 0.190]
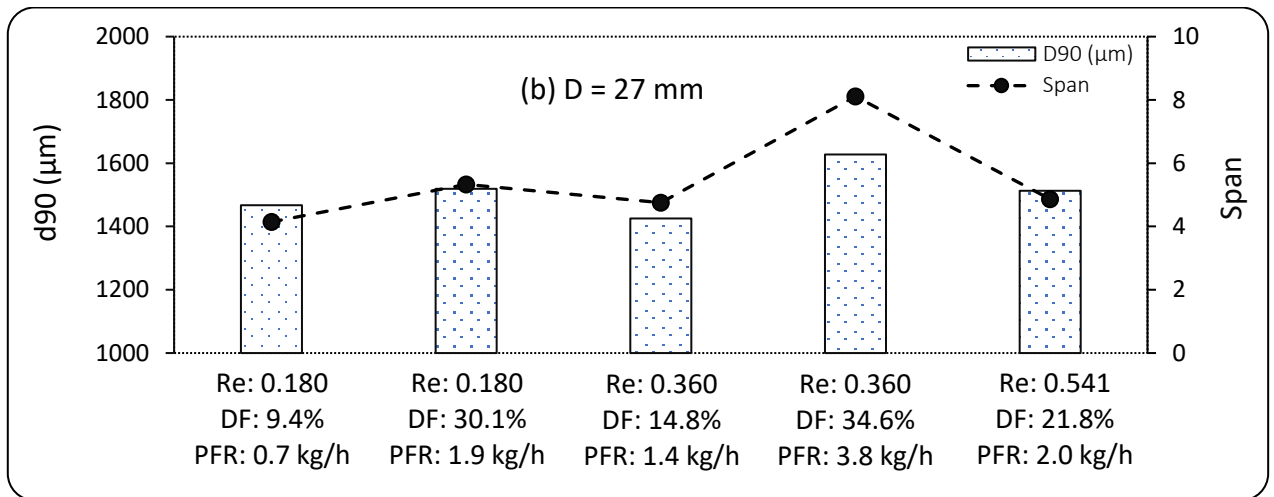
Figure A.13. Effect of Degree of fill (DF) and Reynolds number (Re) on d_{90} and Span with L/S ratio = 26% at (a) D = 18 mm and (b) D = 27 mm [for D = 18 mm, RSE for d_{90} & Span =46.442 & 0.188 and for D = 27 mm, RSE for

A.5 Tree Diagrams for GP-based Symbolic Regression Model

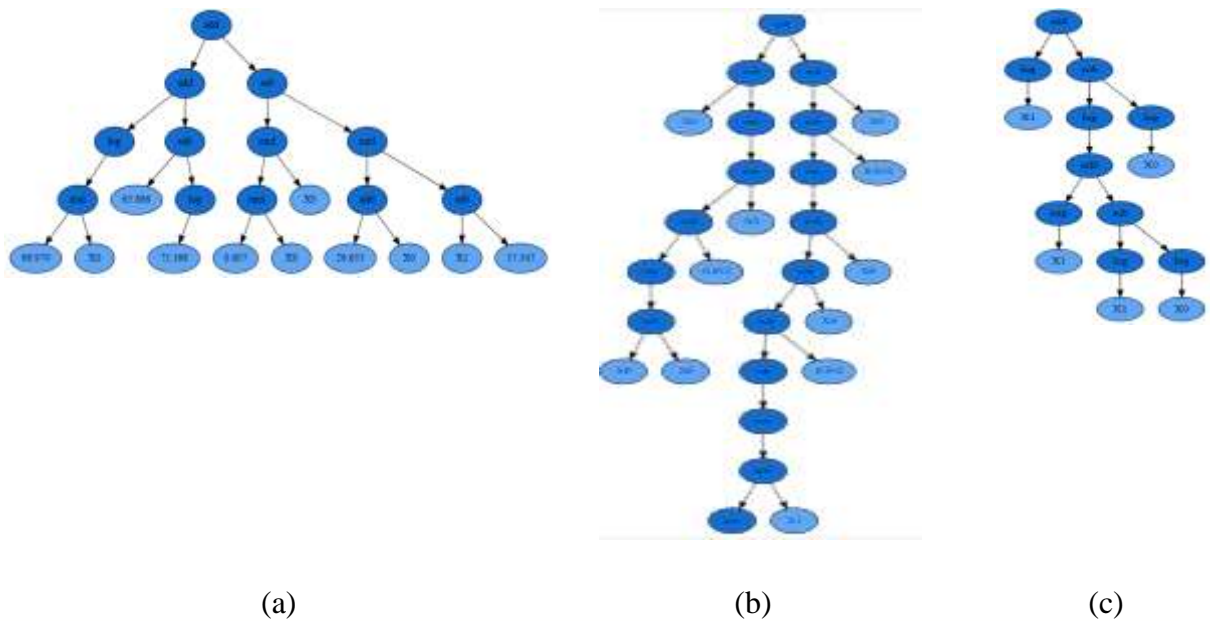(a)   (b)   (c)

Figure A.14. Tree diagrams of GP-based Symbolic regression models for (a) d_{90}, (b) Span, and (c) Fracture strength (FS) for 18 mm TSE [where X_0 = Reynolds number (Re) and X_1 = Péclet number (Pe)]
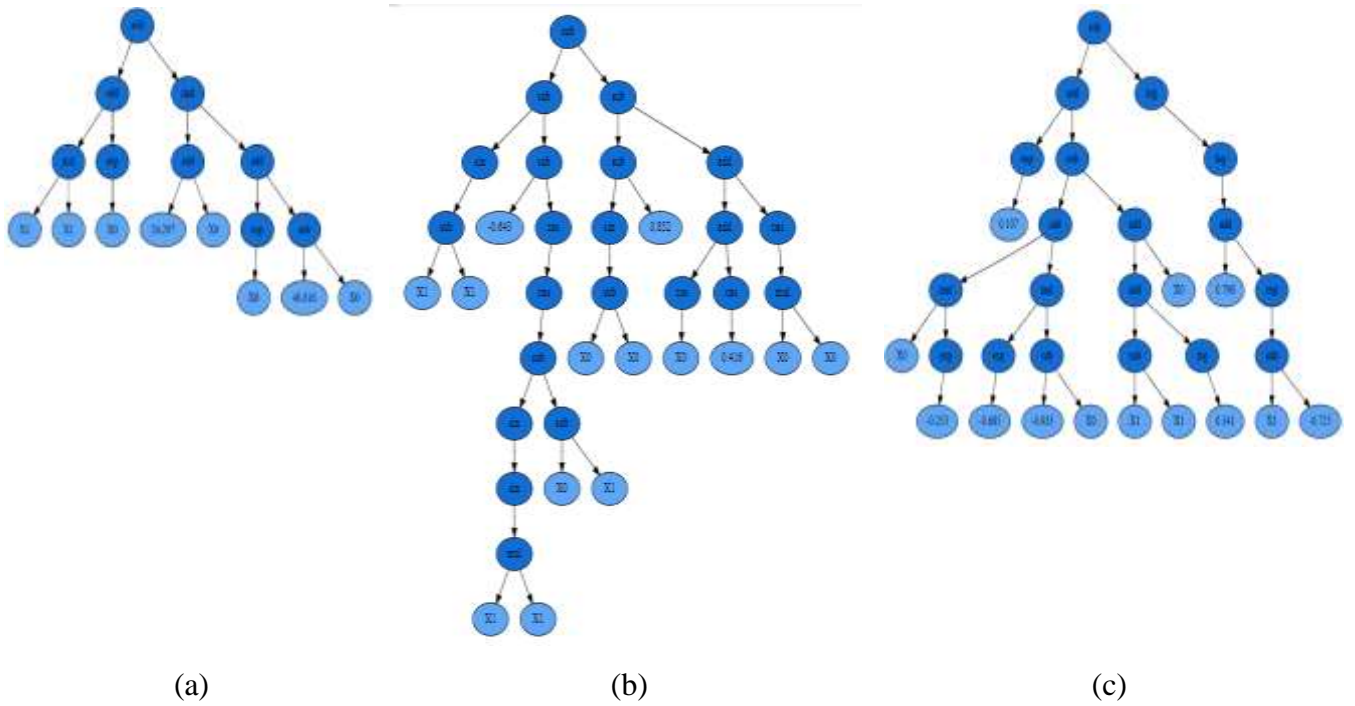
Figure A.15. Tree diagrams of GP-based Symbolic regression models for (a) d₉₀, (b) Span, and (c) Fracture strength (FS) for 27 mm TSE [where X_0 = Reynolds number (Re) and X_1 = Péclet number (Pe)]